UCRL-JRNL-205610

Effects of Model Resolution and Subgrid-Scale Physics on the Simulation of Daily Precipitation in the Continental United States

J. P. Iorio, P. B. Duffy, B. Govindasamy, and S. L. Thompson
Lawrence Livermore National Laboratory
M. Khairoutdinov and D. Randall
Colorado State University

This paper was submitted to: Journal of Climate

July/2004

Effects of Model Resolution and Subgrid-Scale Physics on the Simulation of Daily Precipitation in the Continental United States

J. P. Iorio, P. B. Duffy, B. Govindasamy, and S. L. Thompson
Lawrence Livermore National Laboratory
M. Khairoutdinov and D. Randall
Colorado State University

Corresponding author: P.B. Duffy
pduffy@llnl.gov
tel: 925 422 3722
fax: 925 422 6388

Abstract

We analyze simulations of the global climate performed at a range of spatial resolutions to assess the effects of horizontal spatial resolution on the ability to simulate precipitation in the continental United States. The model investigated is the CCM3 general circulation model. We also preliminarily assess the effect of replacing cloud and convective parameterizations in a coarse-resolution (T42) model with an embedded cloud-system resolving model (CSRM). We examine both spatial patterns of seasonal-mean precipitation and daily-timescale temporal variability of precipitation in the continental United States. For DJF and SON, high-resolution simulations produce spatial patterns of seasonal-mean precipitation that agree more closely with observed precipitation patterns than do results from the same model (CCM3) at coarse resolution. However, in JJA and MAM, there is little improvement in spatial patterns of seasonal-mean precipitation with increasing resolution, particularly in the Southeast. This is owed to the dominance of convective (i.e., parameterized) precipitation in these two seasons. We further find that higher-resolution simulations have more realistic daily precipitation statistics. In particular, the well-known tendency at coarse resolution to have too many days with weak precipitation and not enough intense precipitation is partially eliminated in higher-resolution simulations. However, even at the highest resolution examined here (T239), the simulated intensity of the mean and of high-percentile daily precipitation amounts is too low. This is especially true in the Southeast, where the most extreme events occur. A new GCM, in

which a cloud-resolving model (CSRM) is embedded in each grid cell and replaces convective and stratiform cloud parameterizations, solves this problem, and actually produces too much precipitation in the form of extreme events. However, in contrast to high-resolution versions of CCM3, this model produces little improvement in spatial patterns of seasonal-mean precipitation compared to models at the same resolution using traditional parameterizations. Thus, our results suggest that using an embedded 'Cloud Resolving Model' in a high-resolution GCM might provide the best representation of spatial and temporal variability of midlatitude continental precipitation.

1. Introduction

Some of the most important societal impacts of anthropogenic climate change will likely result from changes in precipitation. These impacts will result from possible changes in the statistics of daily precipitation as well as time-averaged precipitation amounts (IPCC, 2001). In order to choose an appropriate model for studies of future changes in the character of precipitation it is necessary to evaluate these statistical properties in present-day simulations in relation to those of an observed dataset.

A number of recent papers have suggested that the simulated temporal variability of climate models improve at higher spatial resolutions. Many of these studies focused on regional comparisons in which a nested regional climate model was employed to provide high-resolution results. A particular area for these regional model evaluations was the United States, an area with a relatively dense observational network. From this work it has been found that biases in the spatial and temporal variability of precipitation, which are present in coarse-resolution GCMs are often reduced in higher-resolution models (Giorgi et al., 1994; Mearns et al., 1995; Giorgi et al., 1998). Particular findings are discussed below, after which we discuss probable causes for coarse-GCM deficiencies.

Giorgi et al. (1994) employed a regional climate model nested within a global climate model to simulate precipitation in the U.S. They found that in relation to the observations, the global climate model (GENESIS, a modified CCM1 at 4.5° by 7.5° resolution) greatly over predicted (50-70%) the mean precipitation in both the warm (May-Sept.) and cold (Nov. - March) seasons. The regional model, MM4 (60km grid spacing), under predicted the mean rainfall, but only by about 20% in both

seasons. During the cold season, MM4 better represented the magnitude of spatial variability (spatial σ) than the GCM while in the warm season, the opposite was true.

Using similar regional (RCM) and global (GCM) models, Mearns et al. (1995) compared the RCM precipitation to spatial averages of point observations in the Northwest U.S. The RCM reproduced the seasonal cycle of monthly mean precipitation, though only by overcompensating for a lower intensity (mean precipitation on days with precipitation, defined by a selected threshold) with a higher frequency of rainfall. Though the GCM realistically simulated the monthly mean intensity, it produced too many rainy days and as a result overestimated mean precipitation. Mearns et al. (1995) found that the frequency of rain in the RCM and GCM diminished as they increased the defining threshold. Thus both regional and global models tended to produce too many rainy days.

Giorgi et al. (1998) performed comparisons to observed precipitation over the central Plains of the U.S. In this experiment, they employed the CSIRO global climate model at 5° by 5° resolution and an augmented MM4 at 50km as a nested regional model. They found that the RCM better simulated the location of the summer maximum and also captured the rainshadow effects across the western U.S in both summer and winter. The correlation between the observations and the RCM results for the mean climate for each season was much higher than the correlation with the GCM results.

These studies suggest that climate models using coarse spatial resolutions have difficulty representing both the spatial patterns of time-averaged precipitation and the statistics of daily events. Gordon et al. (1992) gave several reasons why GCMs at coarse resolution have difficulty simulating the frequency and magnitude of extreme events in particular. First, models with low horizontal resolution, by definition, can only show large area-averaged rainfall, which precludes them from representing extreme events that occur in small catchments. Also, coarse resolution GCMs may lack the mechanisms, such as ENSO or tropical cyclones that drive many extreme events. We also note that much of GCM-simulated precipitation is produced via semi-empirical parameterizations, which account for sub-grid scale processes. We show below that the coarser the GCM resolution the more the model relies on these parameterizations. Thus, one may suspect that some of the deficiencies in simulated precipitation in coarse resolution GCMs are due to limitations of the subgrid-scale parameterizations.

We evaluate simulated precipitation in the CCM3 global climate model at a range of spatial resolutions. The broad results of most of these simulations have been described elsewhere: Duffy et al. (2003) described the sensitivity of the simulated present climate to horizontal spatial resolution; Govindasamy et al. (2003) describe how the simulated response to increased greenhouse gases depends on model resolution. Here we focus on analyzing the spatial pattern of seasonal-mean precipitation and the statistics of simulated daily precipitation in the continental United States for the present climate regime. This region is selected in part because high-resolution observations of daily precipitation are available there.

We will show that the realism of simulated spatial patterns of seasonal-mean precipitation is strongly dependent on model resolution in DJF and SON, but not in JJA or MAM. These differing sensitivities to model resolution arise because JJA and MAM precipitation is produced primarily by the convective parameterization scheme, whereas DJF and SON precipitation is produced primarily by the model's large-scale mechanism. We find also that the observed statistics of daily precipitation amounts in the U.S. are reproduced more accurately in higher-resolution simulations than at coarse resolution. In particular, the tendency of the CCM3 model at coarse resolution models to have too much precipitation in the form of weak precipitation events and not enough strong precipitation events (a problem shared by other climate models) is greatly relieved by using finer spatial resolutions. Nonetheless, there are obvious limitations in the ability of the CCM3 model to simulate U.S. precipitation even at high resolutions. These arise in part from inadequacies in the model's representation of subgrid scale physical processes. To address these limitations, a new global climate model has been recently developed in which some of the parameterizations of subgrid scale processes have been replaced by an embedded high-resolution cloud-system resolving model known as the "superparameterization." In this 'SP-CAM' model, the problem of undersimulation of extreme precipitation events is eliminated. (In fact, the model produces too much precipitation in the form of extreme daily events.) However, simulated spatial variability of seasonal-mean precipitation is little better than in traditional parameterized models at the same resolution.

2. Description of Model and Simulations

We performed and analyzed a series of present-climate simulations using the CCM3 atmospheric general circulation model, developed at the National Center for Atmospheric Research. We used a

model version known as 'CCM3.10.11 with 3.6.6 physics.' This has the same physics as version 3.6.6, but computational aspects of the model have been modified to allow more reliable and efficient operation on massively parallel computers.

CCM3 is a global spectral model. It uses a hybrid vertical coordinate that is terrain-following at the surface and reduces to a pressure coordinate in the upper atmosphere (Simmons and Sturfing, 1981). As configured here, CCM3 uses 18 levels in the vertical with the model top at 2.9 mb. Important physical processes are represented as described in detail by Kiehl et al. (1998a,b). The CCM3 includes a comprehensive model of land surface processes known as the NCAR Land Surface Model (LSM; Bonan, 1998).

We performed a series of present-climate simulations at different spectral truncations and horizontal grid resolutions. Some of these simulations are described in detail by Duffy et al. (2003). As a basis for comparison to higher-resolution results, we performed simulations at the standard T42 truncation, in which the transform grid has 128x64 grid cells. The horizontal grid dimension is ~300 km. We also performed two simulations at T170 truncation, with 512x256 grid cells (~75 km grid size), and two simulations at T239 truncation (720x360 cells; ~50 km grid size). At the T239 and T170 resolutions, we performed both 'tuned' and 'untuned' cases as described below. All simulations, except T239 AMIP, are forced with observed, monthly-mean climatologically averaged sea-surface temperatures (SSTs). The T239 AMIP model is forced with monthly mean observed SSTs from years 1980-1984. The SSTs are based on an observed dataset at 1° by 1° spatial resolution; these SSTs were interpolated to the grid used in each simulation. In these simulations present-day concentrations of atmospheric greenhouse gases are prescribed (Table 2). In the first part of the results section of the paper (3.1) we also discuss results of CCM3 simulations performed at T85. Salient properties of all simulations discussed here appear in Table 1.

Initial simulations at T170 and T239 used an 'untuned' version of the model. In these simulations, only the time step and diffusion coefficients were changed relative to the T42 model version. (Thus, although we refer to this model version as 'untuned', it was extensively tuned at T42.) In subsequent simulations at T170 and T239, values of some parameters in the cloud and evaporation parameterizations were adjusted in order to minimize biases seen in results of the untuned T170 simulation. This tuning process is described in more detail in Duffy et al. (2003). Only one retuning

was performed; we used the same tuning coefficients in the 'T170 tuned' and 'T239 tuned' simulations. It should be kept in mind that the tuning process we performed at T170 was much less thorough than that performed on the T42 model version. In the results section below, we show both 'tuned' and 'untuned' cases of the T170 and T239. Differences between the two cases were generally negligible in all of the analyses performed.

3. Results

3.1 Spatial Patterns of Seasonal- and Annual- Mean Precipitation

We start by assessing the effect of horizontal spatial resolution on the simulated spatial pattern of annual- and seasonal-mean precipitation in the continental U.S. We compare our model results for time-averaged precipitation to an observed dataset (NOAA, 2003). The observed dataset has a spatial resolution of 0.25°. For all calculations shown for NOAA, we employ the last 10 years from the dataset, 1989-98.

The spatial pattern of annual-mean precipitation appears to be on the whole more realistically simulated at finer spatial resolutions (Figure 1). In some regions, particularly the West, the improvements appear to result largely from better resolution of topography in the finer-resolution simulations. In other regions, however, (notably the Southeast) the improved results at fine resolutions do not seem to be directly related to better representation of topography. Improvements with increasing resolution are also seen in simulated seasonal-mean precipitation, but the degree of improvement varies with season. In DJF and to a lesser extent in SON, the simulated pattern of precipitation improves with increasing resolution; in MAM and JJA, little improvement is seen (Figs 2-5). In JJA, for example, each simulation misplaces westward the location of the summer maximum. This phenomenon is also present in the JJA precipitation field for the mean of all CMIP (Coupled Model Intercomparison Project) models (Coquard et. al, 2003). A region of particular interest for comparison is the Southeast because it comprises a wide area of the heaviest precipitation over the U.S. Here, the precipitation appears to be represented more accurately at finer resolutions in DJF and to an extent SON (Figures 2, 5), but not in other seasons (Figures 3 – 4). As discussed below, this seems to result from the dominance of 'large-scale' precipitation over 'convective' precipitation in DJF and SON, whereas the opposite is true in other seasons.

To quantify how errors in time-averaged simulated precipitation depend on model resolution, we calculated the total RMS error (Equation 1 below) in simulated mean precipitation at each model resolution (Figure 6). Prior to computing this statistic all model results were downscaled to the observed resolution of 0.25°. In DJF and SON, RMS errors decrease systematically as resolution becomes finer. For the other two seasons and the annual mean, the reduction in error between resolutions is not so systematic. For JJA, there is little or no reduction in RMS error beyond T85, while in MAM, there is no apparent relationship between resolution and RMS error. As will be discussed later, we attribute this result to the higher contributions of convective precipitation to the total precipitation field in MAM and SON. Figure 6 suggests that substantial additional reductions in precipitation errors will require improvements to the model physics rather than, or in addition to, further refinement of resolution. We also performed the same analysis with all model results and observations averaged to a T42 grid. On this coarse-grid, the results very closely matched those of Figure 6. Thus, we draw similar conclusions as mentioned above regardless of the spatial scale on which the comparison is performed.

$$\text{Total RMSE} = \left[(1/N) \sum_{n=1}^{N} (f_n - r_n)^2 \right]^{1/2}, \qquad (1)$$

N - Number of grid cells in the U.S.

f_n - Simulated value at grid point 'n'

r_n - Observed value at grid point 'n'

A recurrent theme of our results will be that the CCM3 simulations are better when more of the precipitation is produced by the models 'large-scale' mechanism, rather than by convective parameterization. The 'large-scale' precipitation component is produced when the relative humidity in a model grid cell exceeds 100%. The convective component represents precipitation resulting from subgrid-scale (unresolved) convective events. The model represents these events through parameterizations, which estimate rates of precipitation resulting from condensation occurring in rising subgrid-scale air masses.

As seen in Figure 7, the large-scale component dominates DJF precipitation in all simulations. This is apparently the reason for the substantial improvement with increasing resolution in simulated DJF mean precipitation (Figure 6). The season with the next highest contribution of large-scale precipitation is SON, and thus the improvement with resolution in the mean SON precipitation is also noted in Figure 6. For MAM and JJA mean precipitation, there is little or no improvement with increasing resolution (Figure 6). This is apparently explained by the high percentage of the convective precipitation portion of the field in these seasons (Figure 7). We also noted earlier that all the models had difficulty representing mean precipitation over the Southeast. In the Southeast the convective portion of precipitation is even higher than the nationwide average for all four seasons (almost 100% in JJA). This seems to explain why any improvement noted for the U.S. as a whole is diminished over the Southeast. Figure 7 also shows that in all seasons, the fraction of convective precipitation decreases with increasing resolution. This is expected, because increasing resolution results in more scales of motion being explicitly resolved and thus less reliance on parameterizations.

3.2 Daily Precipitation Statistics

We turn now to looking at some of the statistical properties of simulated daily precipitation amounts, and how they depend on model resolution.

We start by examining mean precipitation intensity, defined as the mean daily precipitation on days having at least 0.1 mm of precipitation. (This threshold is used because it is the traditional minimum measurable amount of daily precipitation). For both JJA and DJF seasons, observed mean precipitation intensities are highest in the Northwest, Southeast, and in the mountains of the west coast (Figures 8a,b and 9a,b). These high intensities are not reproduced in the T42 simulation. For example in the DJF season (Figure 9a), the highest precipitation intensity is around 7 mm/day in the T42 simulation, versus 17 mm/day in observations This is symptomatic of the widespread tendency of coarse-resolution climate models to produce too much precipitation in the form of weak events ('drizzle'), a tendency that has been noted by Mearns et al. (1995). In both seasons, the higher-resolution present-climate simulations appear do a better job of reproducing observed precipitation intensities (Figures 8a and 9a). Notable deficiencies remain, however, particularly in the Southeast, where even the T239 simulations predict precipitation intensities which are only about half of

observed values. This is one symptom of the model's inability to simulate strong daily precipitation amounts in this region; we see below other evidence of this problem.

Because intense precipitation events typically occur on a scale smaller than the grid of any of our simulations, one expects a tendency for increased simulated mean precipitation intensities at finer resolutions. (I.e. averaging the raw precipitation results up to a coarser scale will reduce precipitation intensities.) It is therefore interesting to ask if simulated precipitation intensities in the higher-resolution simulations are closer to observations even if all model and observed data are analyzed on a common spatial grid. In Figures 8b and 9b, therefore, we show results obtained by averaging simulated and observed precipitation to the spatial grid of the T42 model before precipitation intensities were calculated. In both JJA and DJF, precipitation intensities in the higher-resolution simulations are still closer to observed intensities than are simulated intensities from the T42 simulation. Thus we conclude that simulated precipitation intensities in the higher-resolution simulations are not just more detailed but also more accurate than those in the T42 simulation.

Next we examine 99th percentile daily precipitation amounts, which is another measure of the intensity of strong precipitation events. In the T42 simulation, 99th percentile daily precipitation amounts are generally much less than observed values (Figure 10a), especially along the Pacific coast and in the Southeast. This problem appears to be much less severe in finer resolution simulations. However, as with mean precipitation intensities, simulated 99th percentile daily precipitation amounts are too small in the southeast region, even in the T239 simulation. As with simulated precipitation intensities, it is interesting to ask if the improvement seen in the higher resolution simulations persists even if all results are averaged to a common grid before statistics are calculated. In Figure 10b, therefore, we show 99th percentile daily precipitation amounts calculated after raw simulated and observed precipitation data were averaged to the grid of the T42 model. The results of the higher resolution simulations are again more realistic even when analyzed on the grid of the T42 model. Thus, we find more evidence that the higher-resolution simulations are more accurate, as well as more detailed, than the T42 simulation.

To look more generally at the model's ability to simulate the statistics of daily precipitation amounts, we calculated cumulative probability distributions for daily precipitation amounts for the continental U.S. as a whole (Figure 11). All raw results, including observations, were averaged up to the grid of

the T42 model prior to conducting this analysis. The T42 simulation underestimates the strength of high-percentile daily precipitation amounts. (For example, the 99th percentile daily precipitation amount is roughly 40 mm in the NOAA observational data set, but only about 20 mm in the T42 CLIM simulation.) This problem is significantly mitigated in the higher-resolution simulations. In these simulations, daily precipitation amounts for percentiles less than about 99 are still underestimated, but by much less than in the T42 simulation.

The very highest percentile daily precipitation amounts in the T170 and T239 simulations seem to be excessive, although one could question the ability of gridded observations to accurately represent these extremely strong events. In Figure 12, we test this theory by comparing the distribution of daily precipitation amounts in the NOAA gridded observations against NCDC station data (NCDC, 2003). Here we have sub-sampled the NOAA data set to include results only at times and locations where station data are available. As is clear from the figure, the NOAA dataset appears to under predict the intensity of rare precipitation events. This suggests that the gridded data set may be missing some extreme precipitation events.

Another view of the statistics of daily precipitation amounts is shown in Figure 13, which shows the distribution of area-weighted precipitation rates in km^3/day. As in Figure 10, all raw precipitation data were averaged to the T42 grid prior to conducting the analysis. The height of each bar represents the accumulation of individual precipitation events in each precipitation class (0.1-1.0 mm/d, 1-5 mm/d, etc.). This height is the precipitation rate (km/day) x area of grid cell (km^2), summed over all daily precipitation events belonging to that class and then divided by the number of days in the simulation to obtain the daily average. The simulations tend to produce too much precipitation in events < 10 mm/d, which reaffirms the finding of Mearns et al. (1995) that climate models tend to produce too much weak daily precipitation. The T42 simulation drastically underestimates precipitation in daily amounts of 20 mm/d or more. The higher resolution simulations perform better in simulating these large daily precipitation events, but still produce too little precipitation in some of the higher classes.

The majority of precipitation in the weaker precipitation classes is produced via convective adjustment; this proportion decreases in the stronger precipitation classes (Figure 13). Daily precipitation events of 20 mm/day or more are produced primarily through the model's large-scale mechanism. Thus, the improved representation of strong daily precipitation events in the higher-

resolution simulations is owed mainly to the ability of those simulations resolve more scales of motion and thus rely less on the convective parameterization, rather than to any improved performance of the parameterization.

Another commonly used measure of extreme precipitation events are return times for specified daily precipitation amounts. Here we assess the ability of the CCM3 model to simulate return times for daily precipitation amounts of 10 mm, 20 mm, and 40 mm. For a daily precipitation amount of 10 mm, the T42 simulation overestimates return times, most notably in the Southeast, in the mountains of California and in the extreme North-central states (Figure 14a). This problem is reduced in the higher-resolution simulations. However, again in the southeast all simulations overestimate return times for 10 mm of daily precipitation. As with other precipitation statistics, we also examine return times with all precipitation data first averaged to a common spatial grid. Figure 14b shows return times for 10 mm of daily precipitation calculated after all precipitation data were averaged to the grid of the T42 model. Again as with the other precipitation statistics, the results of the higher-resolution simulations are superior to those of the T42 simulation even when analyzed on the grid of the T42 model.

For higher daily precipitation amounts, the T42 model dramatically over predicts return times. For example, in most regions of the U.S. 40 mm of daily precipitation occurs less often than once in ten years in the T42 simulation. By contrast, observed return times in many regions (e.g. the southeast) are less than half a year (Figure 16a), and even at a T42 grid scale are about a year (Figure 16b). The higher-resolution simulations do better than the T42 simulation at simulating 20 mm and 40 mm return times. However, in the southeast, even the T239 simulations substantially over predict return times for 20 mm and 40mm of daily precipitation.

4. Discussion

Our results clearly show that although the model relies less on its convective parameterizations at higher resolutions, even the higher resolution simulations would benefit from improving these parameterizations. For example, even in the high-resolution simulations the dominant precipitation mechanism in MAM and JJA is convective, and in these seasons there is little improvement in the simulated spatial patterns of precipitation with increasing resolution. Similarly, in the high-resolution

simulations amounts of convective precipitation in daily events of 0.1 - 1 mm/day exceed the observed precipitation amount in this precipitation class; thus no degree of improvement to the simulated large-scale precipitation could bring the model into agreement with observations. For these reasons and others, the CCM3 model and climate models generally would benefit from improved representations of subgrid scale processes related to precipitation.

A novel approach to improving the representation of subgrid-scale physical processes was introduced by Khairoutdinov and Randall (2001). They replaced the convective and stratiform cloud parameterizations in the NCAR CAM2 model (the successor to CCM3) with a high-resolution cloud-system resolving model (CSRM), which is embedded within each GCM grid cell. This approach, known as 'super-parameterization' (SP), should in principle have superior predictive capability to traditional parameterizations because it is based more closely on first-principles physics than traditional parameterizations are. A short description of the "superperameterized" model, SP-CAM, is provided below.

The SP-CAM model is based on the Community Atmospheric Model (CAM) version 1.8 developed at NCAR (Collins et al, 2003). The CAM model was used with T42 horizontal resolution (approximately a 2.8 x 2.8° grid), 26 vertical levels with the model top at 3.5 mb, and a semi-Lagrangian dynamical core.

In this model the convective and stratiform cloud parameterizations were replaced by the "Superparameterization" (SP), a 2-D version of 3-D CRM described in detail by Khairoutdinov and Randall (2001). The SP integrates the non-hydrostatic momentum equations using an elastic approximation. The prognostic thermodynamic variables include the liquid/ice water moist static energy, the total non-precipitating water, and the total precipitating water. The cloud water, cloud ice, rain, snow and graupel mixing ratios are diagnosed from the prognostic variables using the partition between liquid and ice phases as a function of temperature. To compute the hydrometeor conversion rates and terminal velocities, a bulk microphysics parameterization is applied.

A copy of the SP was embedded in each of the 8192 grid-columns of the CAM; each SP had a 64 x 24 grid point periodical domain aligned in the west-east direction. The horizontal resolution was 4 km, and the vertical grid levels were located at the same heights as the lowest 24 levels of CAM. As

discussed above, the SP replaces the convective and stratiform cloud parameterizations. The SP was forced by large-scale tendencies updated every CAM time step; the output was its own horizontally averaged tendencies as a feedback to the CAM. Because of unrealistic momentum transport associated with the 2-D dynamics, the SP was not allowed to affect the large-scale momentum. Instead, the SP's horizontal wind components were nudged to the CAM's by relaxing their horizontal averages to the large-scale wind using a one-hour relaxation time scale.

We performed similar analyses of the SP-CAM results as of the CCM3 results. At the time of analysis, less than two years of simulation with SP-CAM had been performed, and the results shown here are based on one year's results. For this reason, and because the SP-CAM model is undergoing rapid development, the SP-CAM results shown here must be regarded as preliminary.

We find that the SP-CAM model eliminates the lack of strong daily precipitation events characteristic of many coarse-resolution GCMs (Figures 11, 13). Figure 13 shows that the SP model in fact undersimulates the amount of precipitation in small events (< 20 mm/d) and oversimulates the amount in intense events (> 20 mm/d). This is the opposite behavior of both the coarse- and fine-resolution versions CCM3.

While the SP approach shows the potential to improve simulations of temporal variability of precipitation, the present SP-CAM results do little to improve simulated spatial variability of precipitation (Figure 6). In terms of spatial variability, the high-resolution CCM3 simulations perform better than both SP-CAM and CCM3 at T42. One reason SP-CAM does not do better is that it is truncated at T42 (~300km). At this scale, topography over the western US is not realistic and thus, the simulated climate, which is orographically sensitive, is also unrealistic. However, a T239 truncation (~50 km) can capture the topographic detail necessary to reproduce the complexity of climate as observed over the western US. Thus, with the mean climate of the west well represented in the two T239 simulations, it is not surprising that they produce the lowest RMS errors over the entire U.S.

5. Conclusions

Increasing the spatial resolution in the CCM3 model leads to more realistic representations of observed present-day precipitation in the continental U.S. Specifically, both the simulated patterns of

seasonal-mean precipitation and the simulated statistics of daily precipitation amounts are improved at finer spatial resolutions. In regard to the spatial patterns of seasonal-mean precipitation, the RMS error improves with resolution annually and for all seasons, but improvements are limited in JJA and MAM. In those two seasons, the convectively-produced precipitation dominates the simulated precipitation field, apparently leading to relatively small improvement with increased resolution. In the Southeast, this component dominates most strongly and thus in this region, one finds the weakest improvement with resolution. In DJF and SON, precipitation is predominantly large-scale, and simulated spatial patterns of precipitation improve substantially with increasing resolution.

With regard to the ability to simulate the statistics of daily precipitation amounts, there is substantial improvement from T42 to the T170 and T239 simulations. Some improvement is still apparent even if the raw precipitation data are averaged onto the T42 grid before statistics are calculated. However, all the CCM3 simulations underestimate the intensity of rare precipitation events in the Southeast, the part of the U.S. where the strongest extreme events occur. The distribution of simulated daily area-weighted precipitation rates improves at the higher spatial resolutions; however, even at high-resolution, CCM3 has too much precipitation in lighter amounts and too little in larger amounts.

Despite improvements with increasing resolution, inadequacies in the parameterized "convective" component of precipitation limit the ability of CCM3 to accurately simulate precipitation. This applies to both the spatial pattern of seasonal-mean precipitation and the statistics of daily precipitation amounts in the U.S. In the case of seasonal-mean precipitation, the limited improvement with resolution in MAM and JJA appears to be due to the predominance of convective precipitation in these seasons. In the case of daily precipitation amounts, it appears that inadequacies in the convective parameterizations contribute to the over-abundance of precipitation in the form of weak events, and lack of precipitation in the form of extreme events, particularly in the Southeast.

A new model, the 'super-parameterized' (SP) version of the NCAR CAM model, addresses shortcomings in traditional representations of convective precipitation by replacing the convective and stratiform cloud parameterizations with a high-resolution embedded 2-dimensional cloud-system resolving model (CSRM). In preliminary results with this model, the problem of undersimulation of extreme precipitation events is completely eliminated. (In fact, this model overproduces precipitation in the form of strong daily events.)

Although the SP-CAM model shows the potential to produce a more realistic temporal variability, high-resolution GCMs, with conventional parameterizations, were superior at representing the spatial variability of seasonal-mean precipitation. This suggests that a high-resolution GCM with a 'super-parameterization' might be able to realistically represent both spatial and temporal variability of simulated precipitation. As a consequence, such a model could be used to foresee the changes in the character of precipitation under an increased greenhouse climate. This information could play a role in dictating future social and economic policies for climate change.

Acknowledgements

This work was performed under the auspices of the U.S. Department of Energy primarily by the Lawrence Livermore National Laboratory under contract No. W–7405-Eng-48. Additional support was provided by the Office of Biological and Environmental Research's Global Change Education Program, financially backed by the Oak Ridge Institute for Science and Education. We would like to thank all of the contributors to this work, especially the developers of the Climate Data Analysis Tools (CDAT) software used to perform our analyses. This software was provided at http://esg.llnl.gov/cdat/. Those developers who acted as support during the analysis were Charles Doutriaux, Jennifer Aquilino and Bob Drach of the Program for Climate Model Diagnosis and Intercomparison (PCMDI).

References

Bonan G (1998) The Land Surface Climatology of the NCAR Land Surface Model Coupled to the NCAR Community Climate Model. *J. Climate, 11*: 1307-1326

Boville, B A, and P R Gent (1998). The NCAR climate system model, version one, *J. Climate*, *11*, 1115-1130.

Collins et al. (2003). Description of the NCAR Community Atmospheric Model (CAM2). Technical Report, National Center for Atmospheric Research, Boulder, CO, 171 pp.

Coquard, J, Duffy PB, Taylor K, Santer BD (2003). Simulations of Western U.S. Surface Climate in 15 Global Climate Models. In preparation.

Duffy, PB and B Govindasamy. High resolution simulations of global climate, Part 1: Simulations of the present climate, submitted to *Climate Dynamics*. In press.

Govindasamy B, PB Duffy and J Coquard. High resolution simulations of global climate, Part 2: Effects of increased greenhouse gases, submitted to *Climate Dynamics*. In press.

Giorgi F, Brodeur CS, Bates GT (1994). Regional Climate Change Scenarios over the United States Produced with a Nested Regional Climate Model. *J. Climate, 7*: 375-399.

Giorgi F, Shields C, Mearns LO, McDaniel L (1998). Regional Nested Model Simulations of Present Day and 2xCO_2 Climate over the Central Plains of the U.S. Climate Change, 40: 457-493.

Gordon HB, Whetton PH, Pittock AB, Fowler AM, Haylock MR (1992). Simulated changes in daily rainfall intensity due to the enhanced greenhouse effect: implications for extreme rainfall events. *Climate Dynamics, 8*: 83-102.

IPCC, 2001. Climate Change 2001: The Scientific Basis. Contributions of Working Group I of the Third Assessment Report of the Intergovernmental Panel on Climate Change. 881 pp.

Khairoutdinov, M. F., and D. A. Randall, 2001: A Cloud Resolving Model as a Cloud Parameterization in the NCAR Community Climate System Model: Preliminary Results. Geophys. Res. Lett., 28, 3617-3620.

Khairoutdinov, MF, and DA Randall (2003): Cloud resolving modeling of the ARM Summer 1997 IOP: Model formulation, results, uncertainties, and sensitivities. *J. Atmos. Sci., 60*: 607-625.

Kiehl JT, Hack JJ, Bonan BG, Boville BA, Williamson DL, Rasch P (1998a). The National Center for Atmospheric Research Community Climate Model: CCM3. *J. Climate, 11*: 1131-1149.

Kiehl JT, Hack JJ, Hurrell J (1998b). The Energy budget of the NCAR Community Climate Model: CCM3. *J. Climate, 11*: 1151-1178.

Kittel, T.G.F., N.A. Rosenbloom, T.H. Painter, D.S. Schimel, and VEMAP Modeling Participants. 1995. The VEMAP integrated database for modeling United States ecosystem/vegetation sensitivity to climate change. *Journal of Biogeography 22*: 857-862.

McAvaney, BJ et al. Climate Change 2001: The Scientific Basis. Contributions of Working Group I of the Third Assessment Report of the Intergovernmental Panel on Climate Change. Chapter 8, pp.471-523.

Mearns, LO, Giorgi F, McDaniel L, Shield C (1995). Analysis of daily variability or precipitation in a nested regional climate model: comparison with observations and doubled CO_2 results. *Global and Planetary Change, 10*: 55-78.

NOAA (2003). CPC US Unified (0.25° x 0.25° Daily) Precipitation data provided by the NOAA-CIRES Climate Diagnostics Center, Boulder, Colorado, USA, from their Web site at http://www.cdc.noaa.gov/.

NCDC (2003). Global Surface Summary of Day (includes daily precipitation). http://www4.ncdc.noaa.gov/cgi-win/wwcgi.dll?wwAW~MP~F.

Simmons AJ, Sturfing R (1981). An energy and angular-momentum conserving finite-difference scheme, hybrid coordinates and medium-range weather prediction. ECMWF Technical Report No. 28, 68pp

Figure 1. Annual mean precipitation simulated by the CCM3 atmospheric climate model at three different spatial resolutions and in an observational data set.

Figure 2. The same as Figure 1, except showing wintertime (DJF) precipitation.

Figure 3. The same as Figure 1, except showing springtime (MAM) precipitation.

Figure 4. The same as Figure 1, except showing summertime (JJA) precipitation.

Figure 5. The same as Figure 1, except showing autumn (SON) precipitation.

Figure 6. RMS errors in simulated seasonal precipitation in United States. Results are shown for the CCM3 model at T42, 85, T170, and T239 truncations. Also included is the result for the SP-CAM model ('SP'), which is discussed later. We calculated RMS errors relative to the NOAA observational data set on that dataset's spatial grid. The x-coordinate is the number of model grid cells in the longitudinal direction.

Figure 7. The fraction of seasonal- and spatial-mean precipitation produced by the convective parameterization in our CCM3 simulations. X-coordinate is the number of model grid cells in the longitudinal direction.

Figure 8a. Mean daily precipitation intensities for the JJA season (precipitation on days having > 0.1 mm of precipitation) as simulated by the CCM3 atmospheric model at spectral truncations of T42

(~300 km grid size), T170 (~75 km grid size), T239 (~50 km grid size) and in a gridded observational data set.

Figure 8b. Same as Figure 8a, but with all datasets averaged to a T42 grid before statistics were calculated.

Figure 9a. Same as Figure 8a, but for the DJF season.

Figure 9b. Same as Figure 8b, but for the DJF season.

Figure 10a. 99th percentile daily precipitation amounts, as simulated by the CCM3 atmospheric model at spectral truncations of T42 (~300 km grid size), T170 (~75 km grid size), T239 (~50 km grid size) and in the NOAA gridded observational data set.

Figure 10b. Same as Figure 10a, but with all datasets averaged to a T42 grid.

Figure 11. Cumulative probability distribution for daily precipitation amounts in United States. Curves show the amount of daily precipitation (horizontal axis) of a given percentile (vertical axis). All precipitation data were averaged to the grid of the T42 mode prior to performing this analysis. Included with the CCM3 simulations is the result for the SP-CAM model ('T42 SP'), which is discussed in Section 4.

Figure 12. As in Figure 11, but for only NOAA and NCDC station data. Only those NOAA grid cells that overlapped a station are included in the NOAA distribution. For each corresponding grid cell, a single station was chosen (that station nearest in elevation to the elevation of the corresponding NOAA grid cell) to be included in the NCDC distribution

Figure 13. The distribution of area-weighted precipitation rates as simulated by 5 versions of the CCM3 and in the NOAA gridded observational dataset. Also shown are results for the SP-CAM model ('T42 SP'), which is discussed in Section 4. The height of each bar is the total area-weighted precipitation rate (precipitation rate x grid cell area) for daily events in each precipitation class (0.1 – 1 mm/day, 1 – 5 mm/day, etc.) The hatched section of each bar represents the amount of convective

(as opposed to large-scale) precipitation. Simulated and observed precipitation data were averaged to the spatial grid of T42 (~300km) before conducting the statistical analysis.

Figure 14a. Return times for 10 mm of daily precipitation, as simulated by the CCM3 atmospheric model at spectral truncations of T42 (~300 km grid size), T170 (~75 km grid size), T239 (~50 km grid size) and in a gridded observational data set. White indicates return times < 10 days.

Figure 14b. Same as Figure 14a, but with all datasets averaged to a T42 grid.

Figure 15a. Return times for 20 mm of daily precipitation, as simulated by the CCM3 atmospheric model at spectral truncations of T42 (~300 km grid size), T170 (~75 km grid size), T239 (~50 km grid size) and in a gridded observational data set. Gray indicates that an event of this magnitude never occurs in the model simulation or observations.

Figure 15b. Same as Figure 15a, but with all datasets averaged to a T42 grid.

Figure 16a. Return times for 40 mm of daily precipitation, as simulated by the CCM3 atmospheric model at spectral truncations of T42 (~300 km grid size), T170 (~75 km grid size), T239 (~50 km grid size) and in a gridded observational data set.

Figure 16b. Same as Figure 16a, but with all datasets averaged to a T42 grid.

Simulation Name	T42	T85	T170 CLIM (untuned)	T170 TUNE2 (tuned)	T239 AMIP (untuned)	T239 CLIM (tuned)
Period simulated	present	present	present	present	1980-1984	present
Truncation	T42	T85	T170	T170	T239	T239
Tuning performed at	T42	T42	T42	T170	T42	T170
Spinup period	25 mos.	25 mos.	25 mos.	15 mos.	13 mos.	68 mos.
Years analyzed	10	10	10	5	5	11
SST forcing	Climatology	Climatology	Climatology	Climatology	AMIP	Climatology
CCM3 Initial Conditions	End of T42 sim.	End of T42 sim.	End of T42 control	End of T170 untuned sim.	End of T42 sim.	End of T239 AMIP sim.
LSM initial conditions	idealized	idealized	idealized	End of T170 untuned sim.	idealized	End of T239 AMIP sim.

Table1: Characteristics of simulations performed and analyzed here.

	CO_2 (ppmv)	CH_4 (ppbv)	N_2O (ppbv)	CFC-11 (pptv)	CFC-12 (pptv)
1xCO_2	355	1714	311	280	503

Table 2: Concentrations of greenhouse gases used in simulations

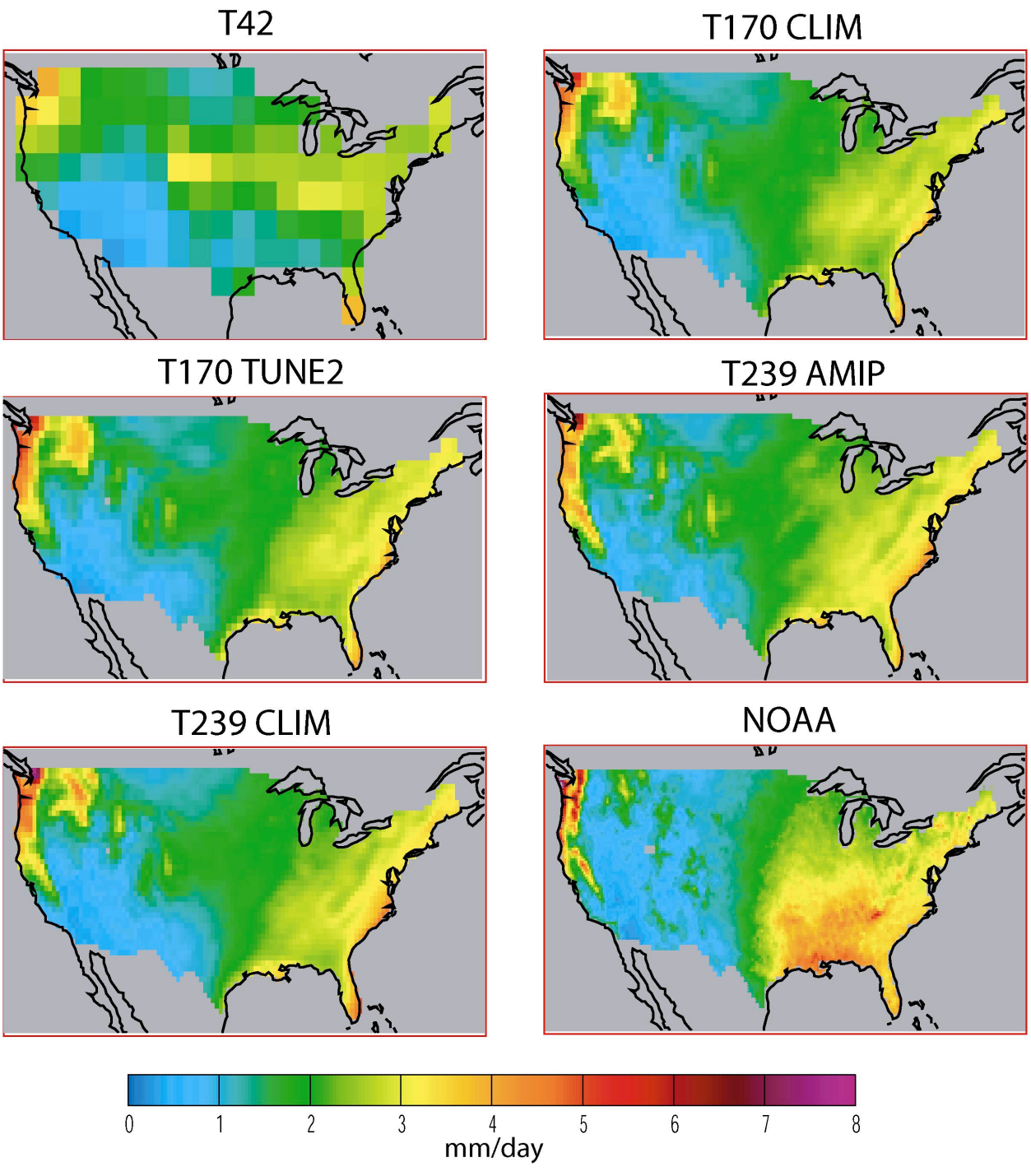
T42
T170 CLIM
T170 TUNE2
T239 AMIP
T239 CLIM
NOAA
0
1
2
3
4
5
6
7
8
mm/day

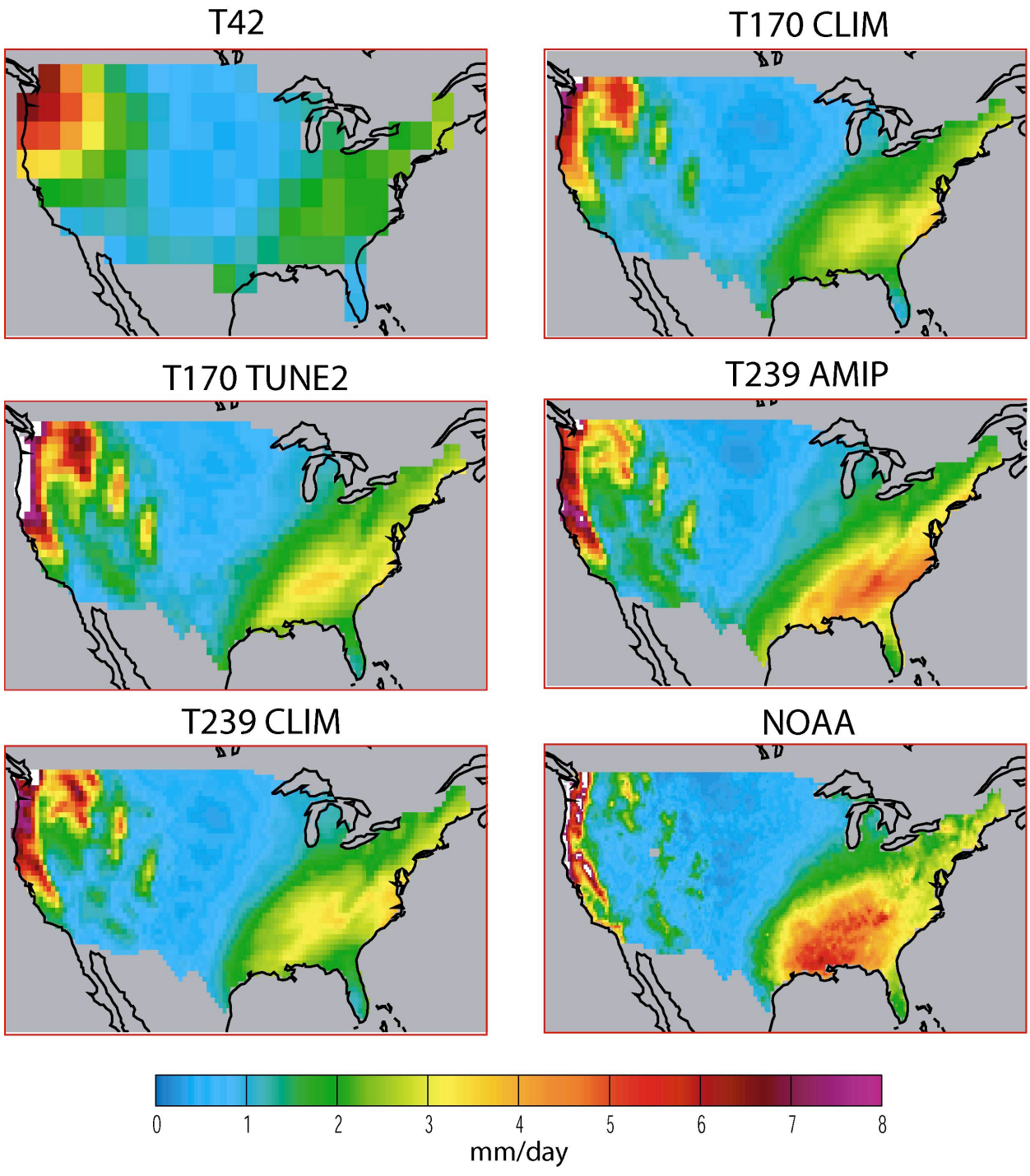
T42
T170 CLIM
T170 TUNE2
T239 AMIP
T239 CLIM
NOAA
0
1
2
3
4
5
6
7
8
mm/day

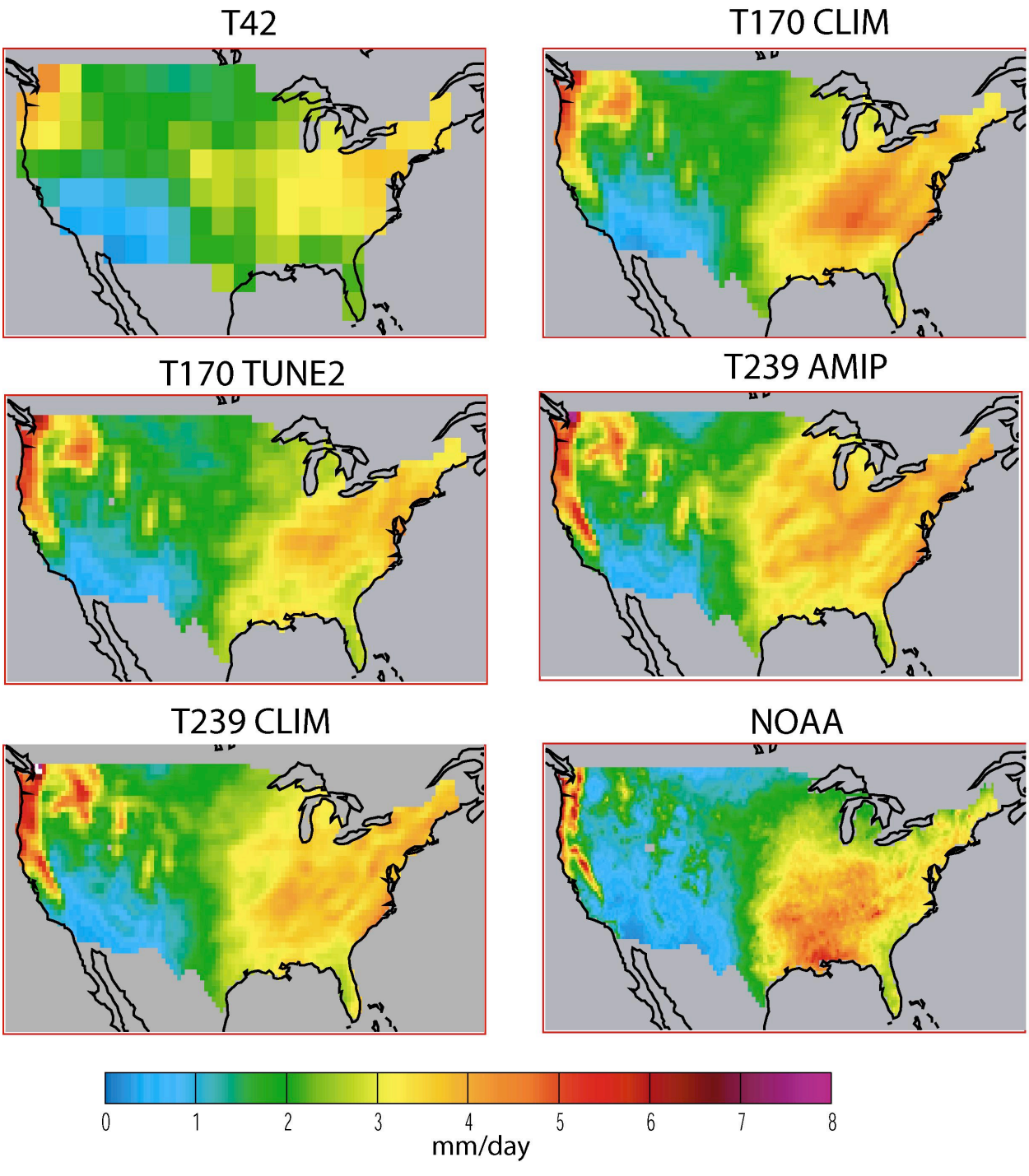
T42
T170 CLIM
T170 TUNE2
T239 AMIP
T239 CLIM
NOAA
0
1
2
3
4
5
6
7
8
mm/day

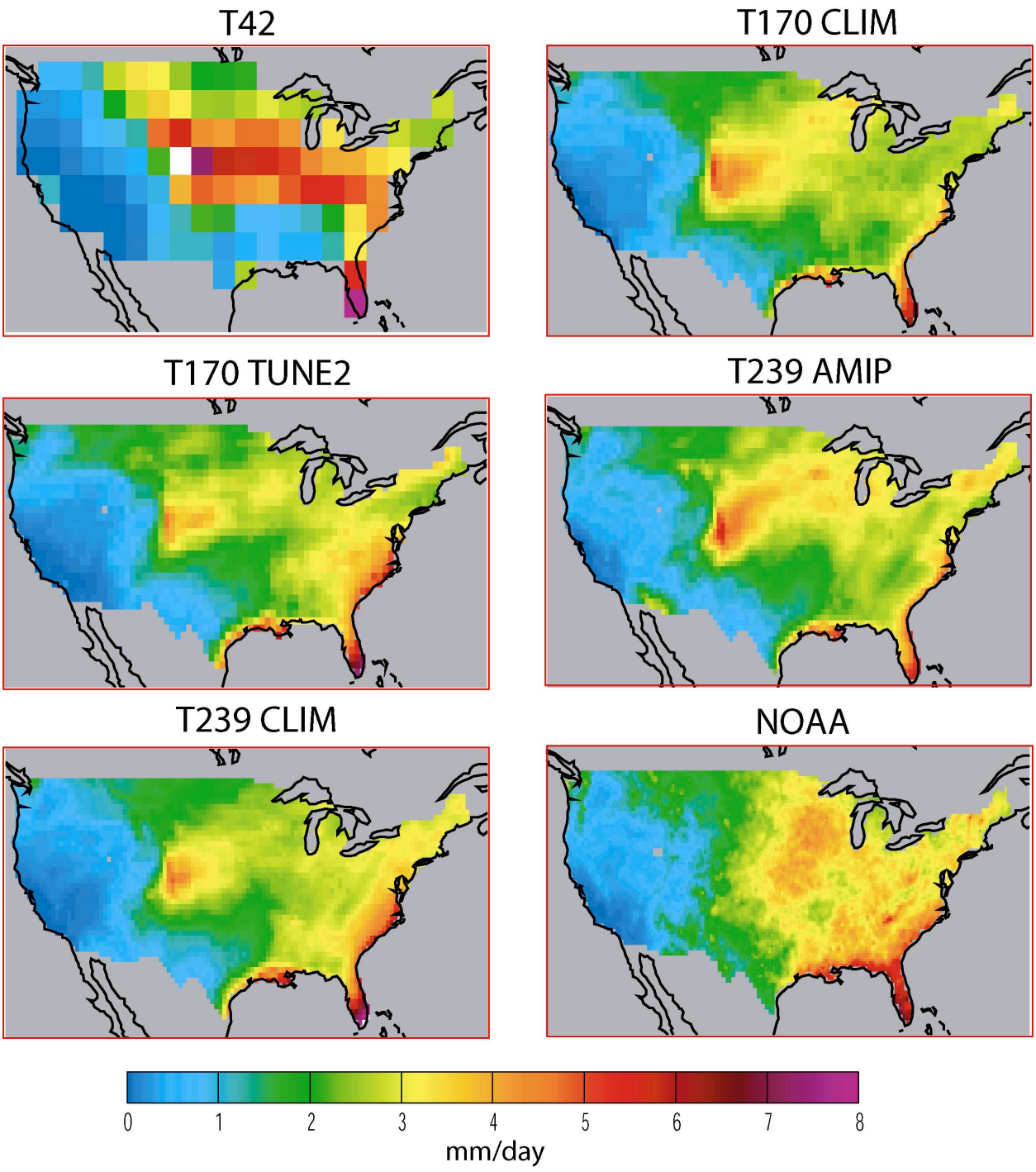
T42
T170 CLIM
T170 TUNE2
T239 AMIP
T239 CLIM
NOAA
0
1
2
3
4
5
6
7
8
mm/day

.

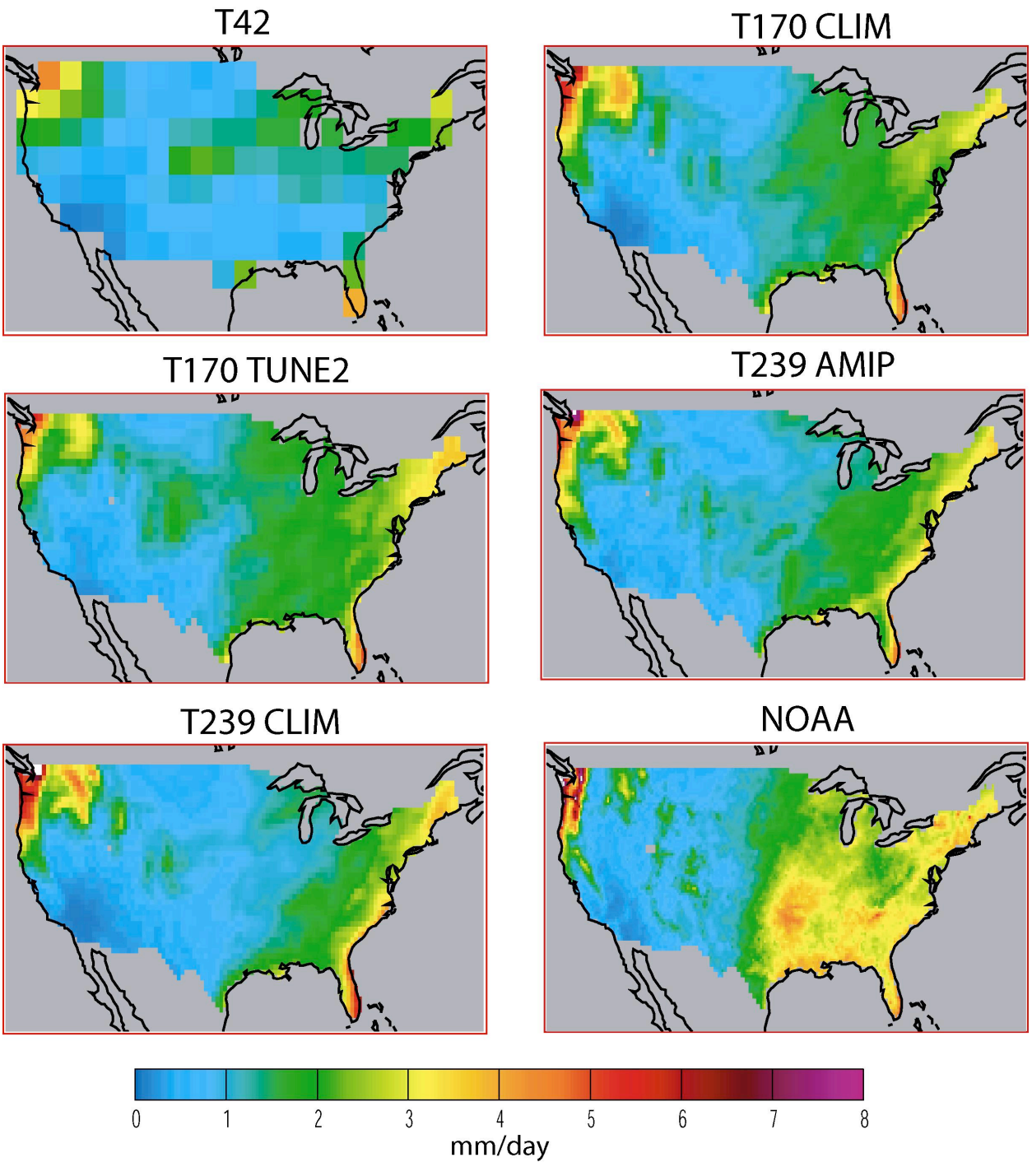
T42
T170 CLIM
T170 TUNE2
T239 AMIP
T239 CLIM
NOAA
0
1
2
3
4
5
6
7
8
mm/day

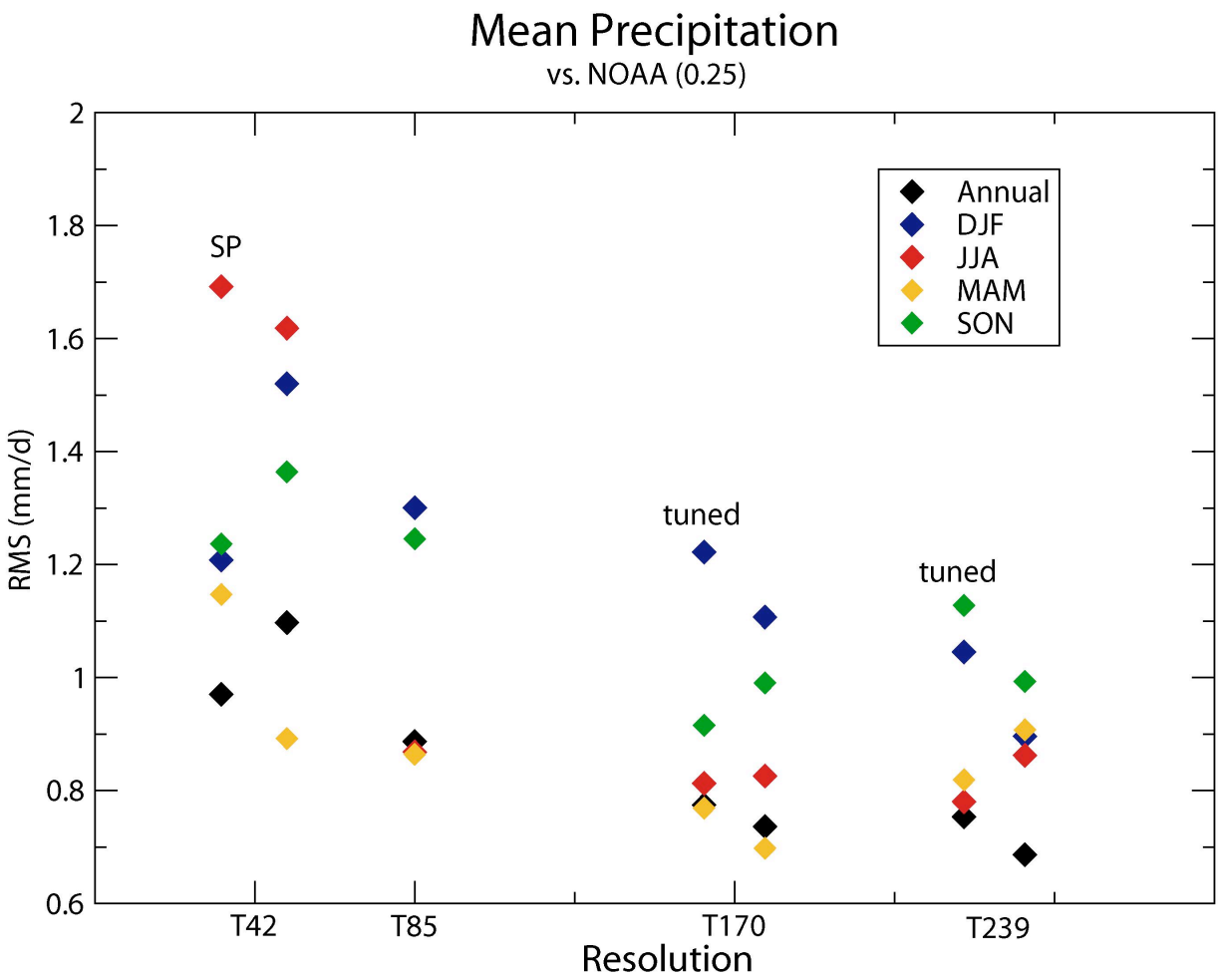
Mean Precipitation
vs. NOAA (0.25)
RMS (mm/d)
2
1.8
1.6
1.4
1.2
1
0.8
0.6
SP
tuned
tuned
Annual
DJF
JJA
MAM
SON
T42
T85
T170
T239
Resolution

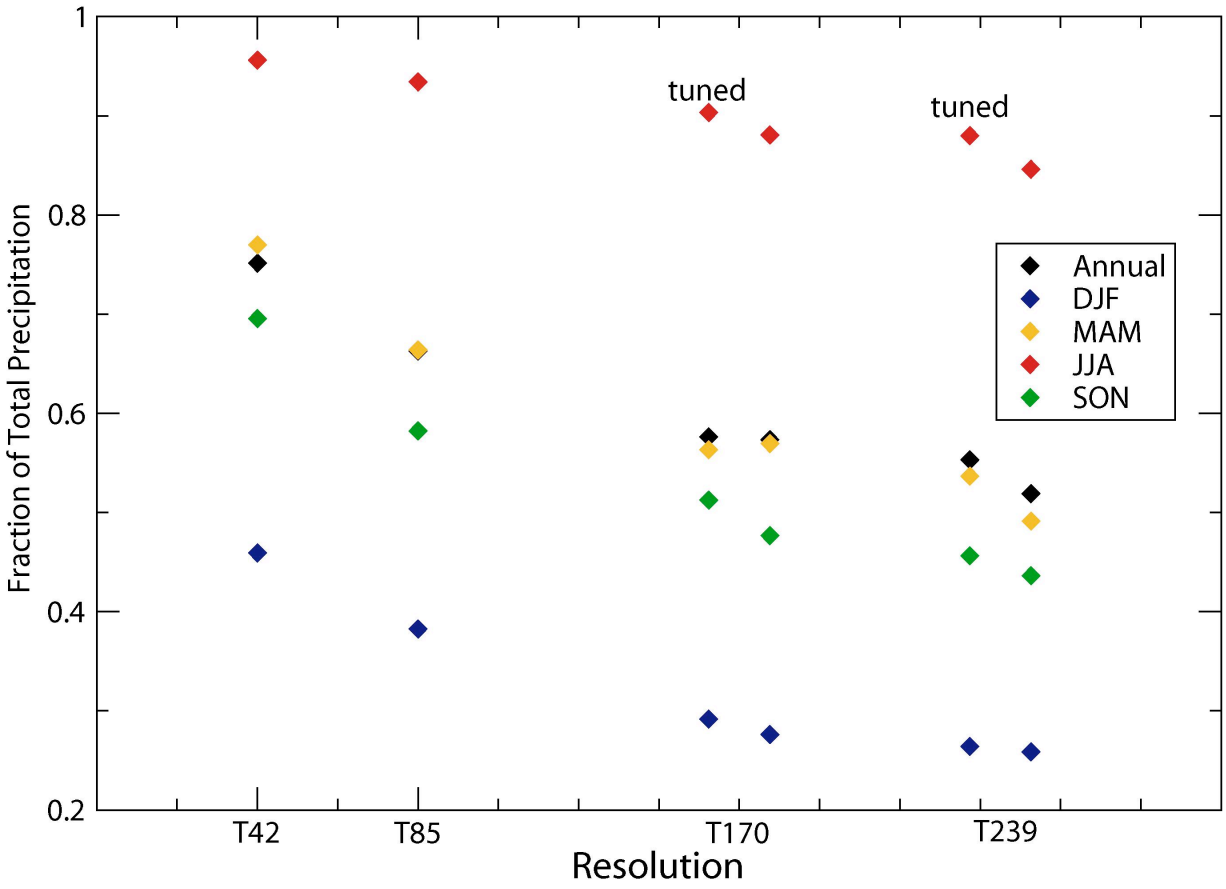
1
0.8
0.6
0.4
0.2
Fraction of Total Precipitation
tuned
tuned
Annual
DJF
MAM
JJA
SON
T42
T85
T170
T239
Resolution

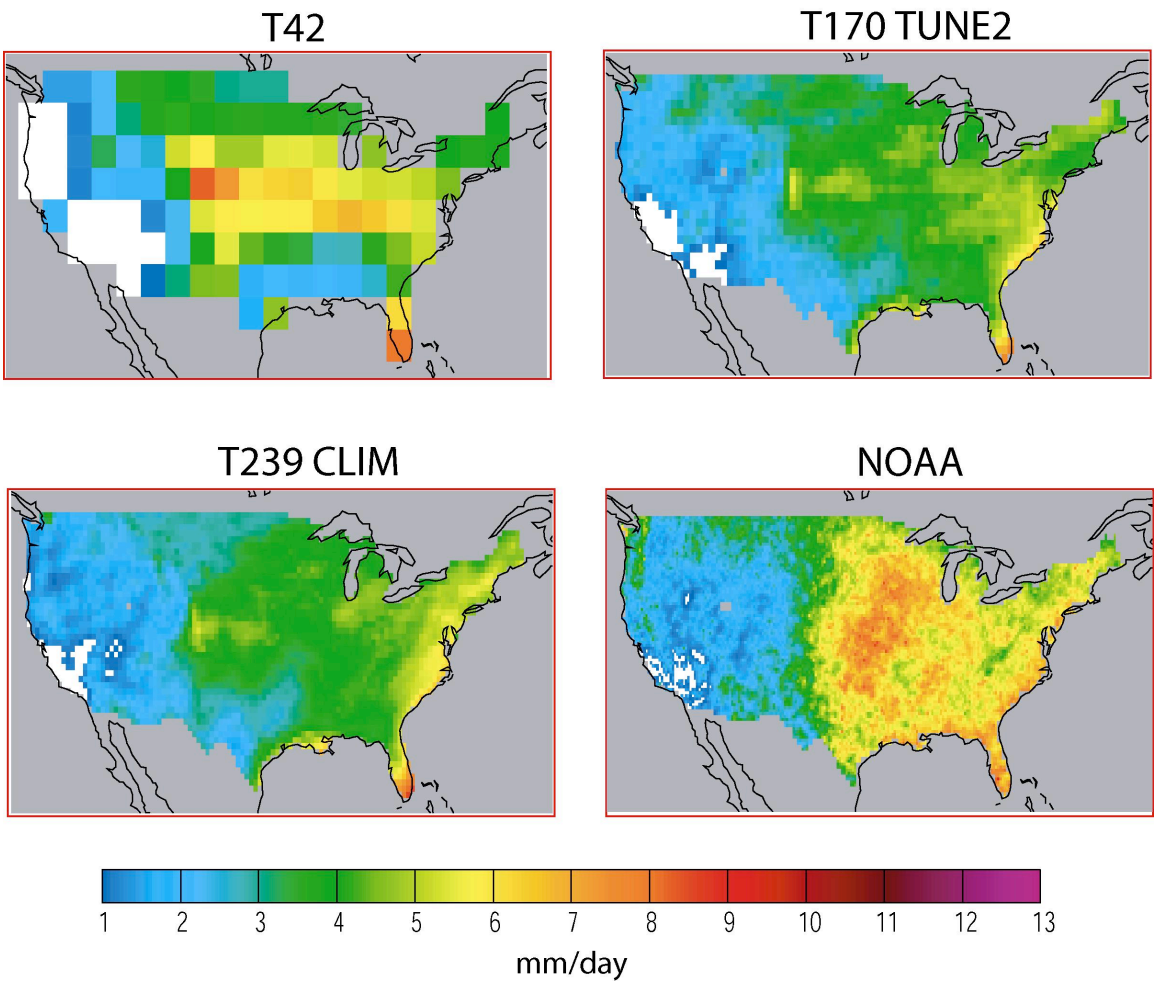
T42
T170 TUNE2
T239 CLIM
NOAA
1
2
3
4
5
6
7
8
9
10
11
12
13
mm/day

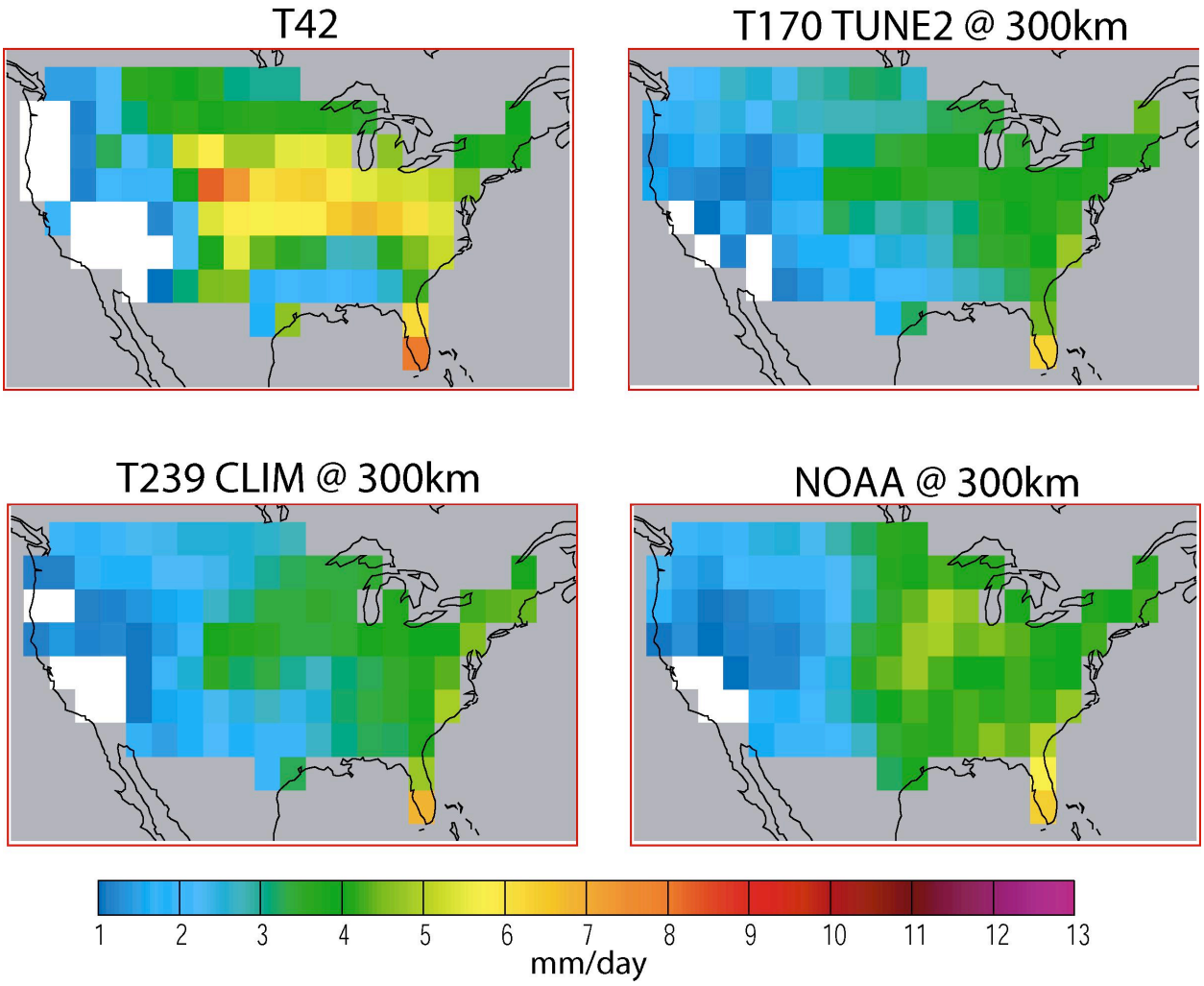
T42
T170 TUNE2 @ 300km
T239 CLIM @ 300km
NOAA @ 300km
1
2
3
4
5
6
7
8
9
10
11
12
13
mm/day

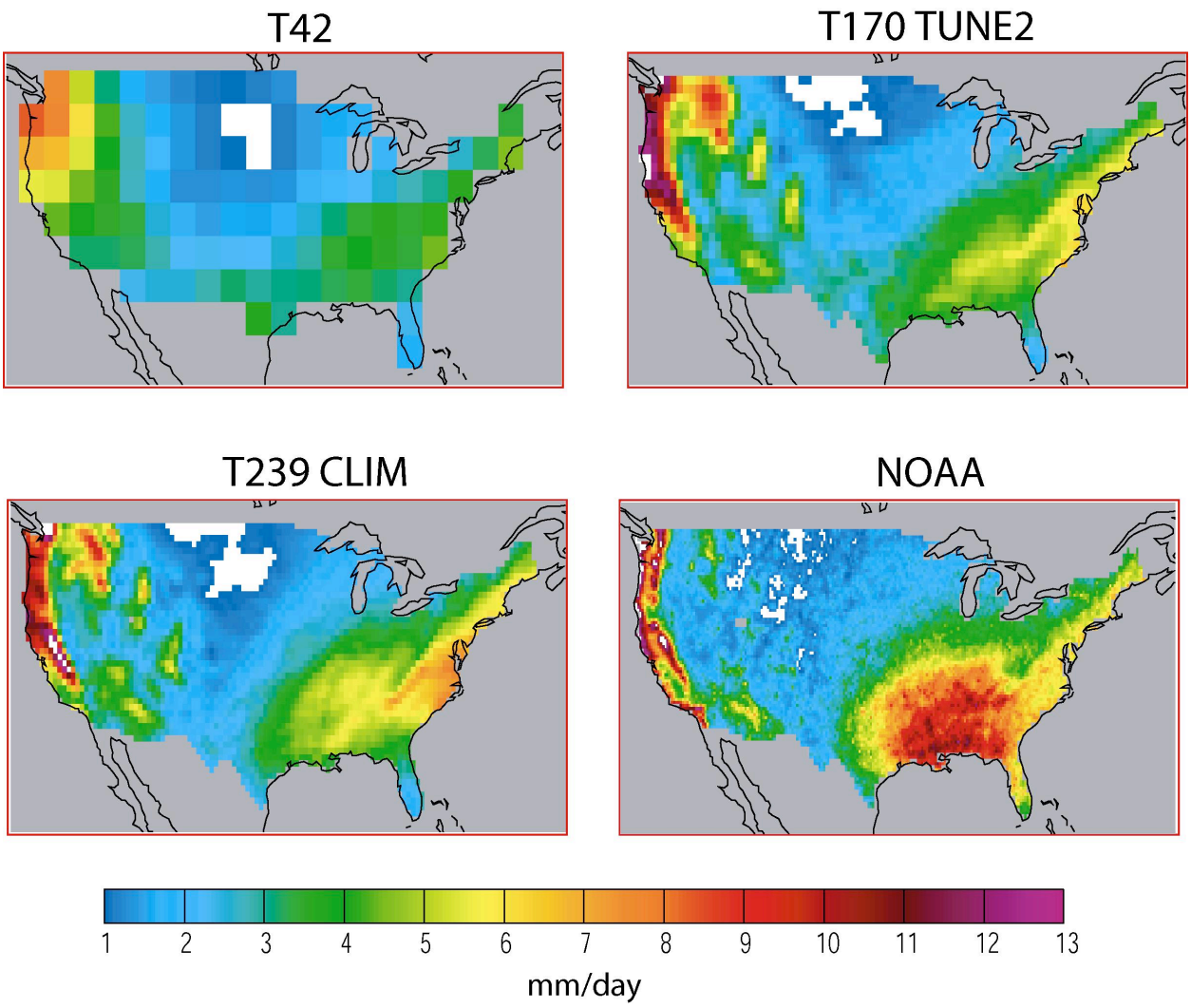
T42
T170 TUNE2
T239 CLIM
NOAA
1
2
3
4
5
6
7
8
9
10
11
12
13
mm/day

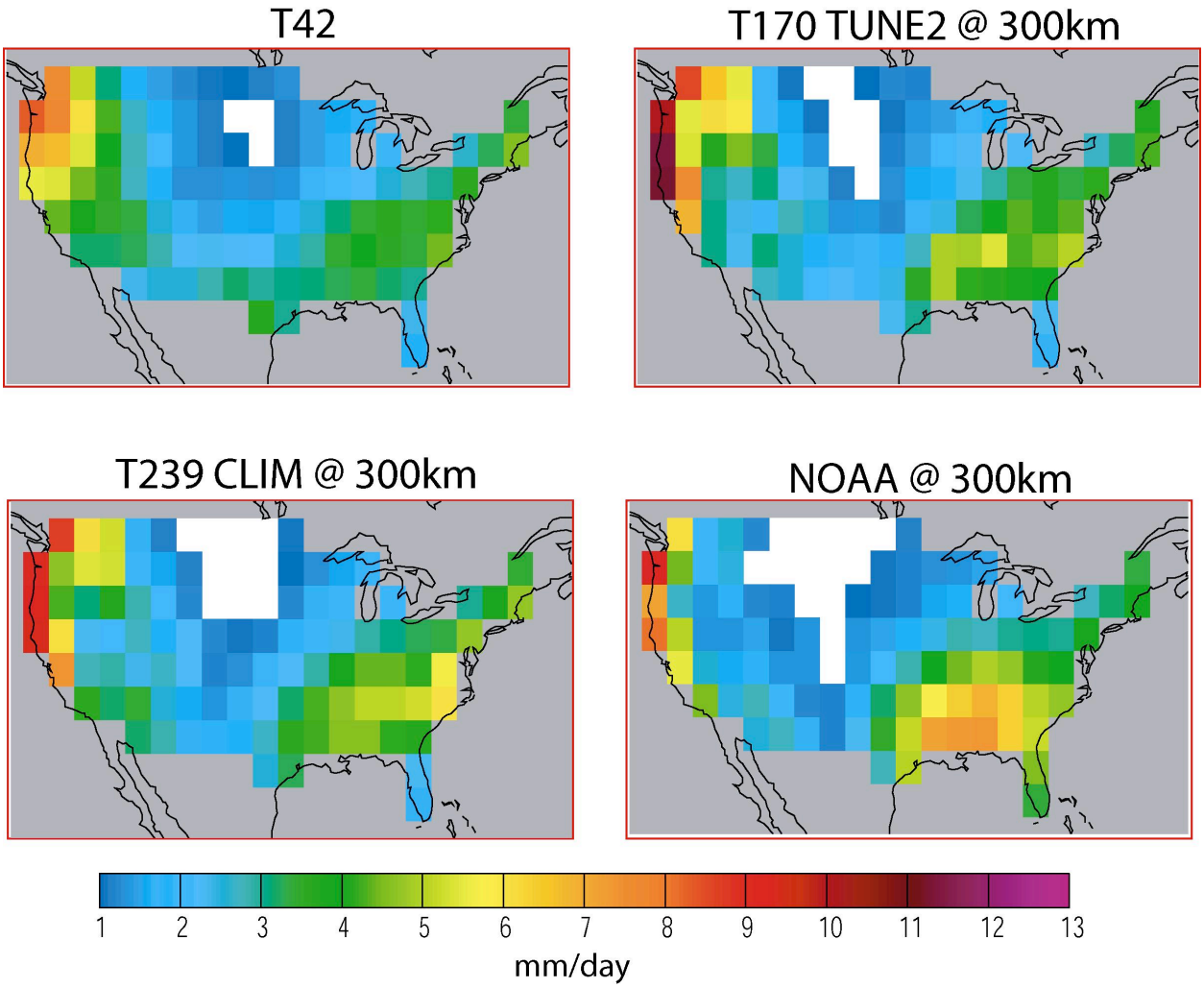
T42
T170 TUNE2 @ 300km
T239 CLIM @ 300km
NOAA @ 300km
1
2
3
4
5
6
7
8
9
10
11
12
13
mm/day

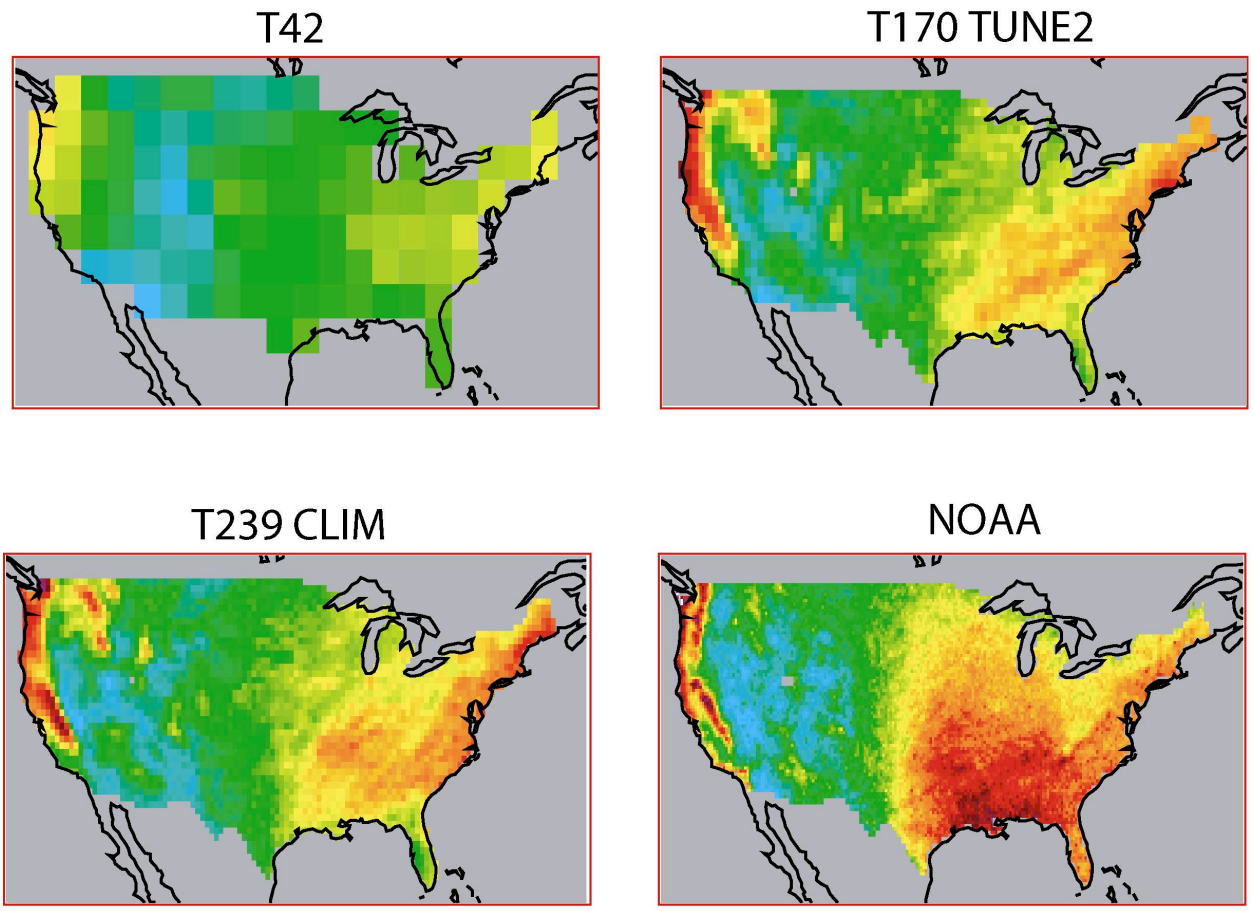
T42
T170 TUNE2
T239 CLIM
NOAA
0
5
10
15
20
25
30
35
40
45
50
55
60
65
mm/day

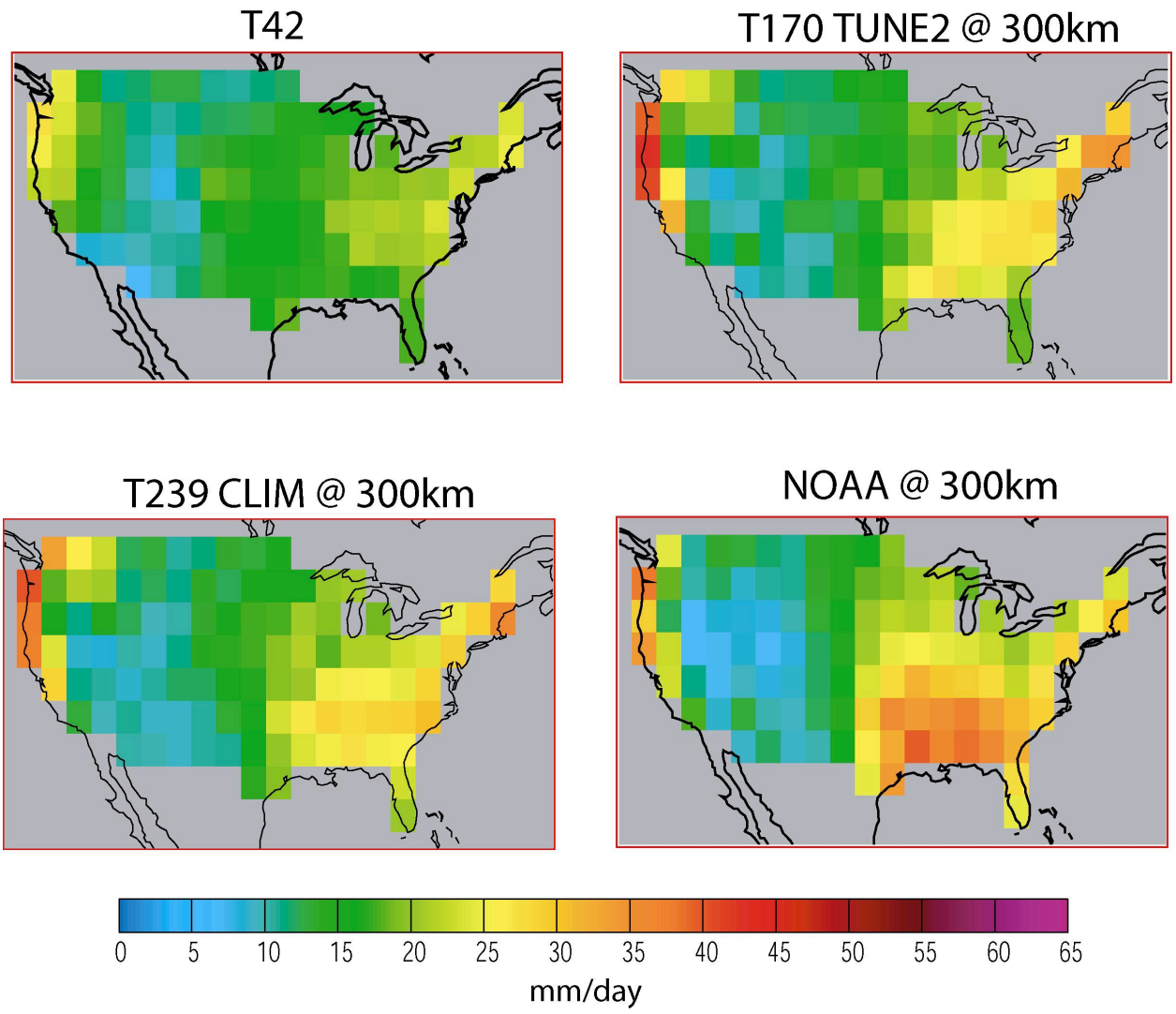
T42
T170 TUNE2 @ 300km
T239 CLIM @ 300km
NOAA @ 300km
0
5
10
15
20
25
30
35
40
45
50
55
60
65
mm/day

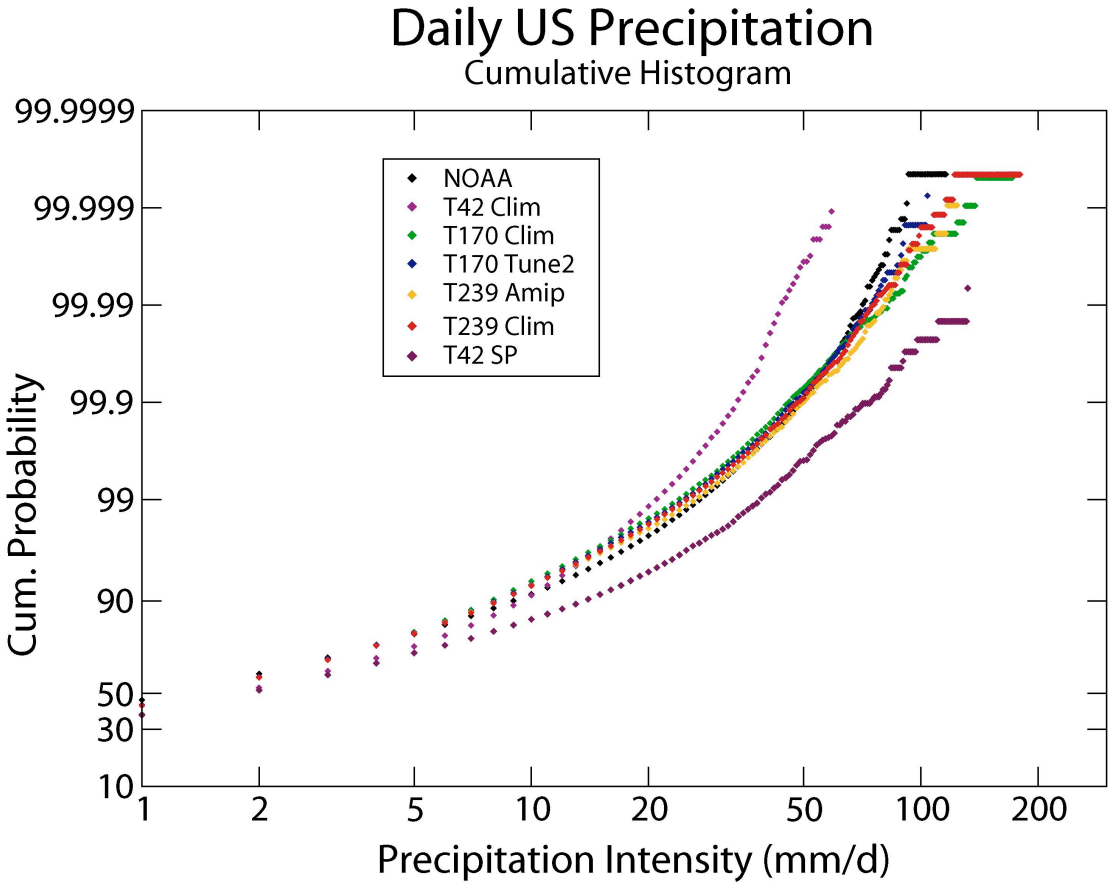
Daily US Precipitation
Cumulative Histogram
NOAA
T42 Clim
T170 Clim
T170 Tune2
T239 Amip
T239 Clim
T42 SP
Cum. Probability
99.9999
99.999
99.99
99.9
99
90
50
30
10
1
2
5
10
20
50
100
200
Precipitation Intensity (mm/d)

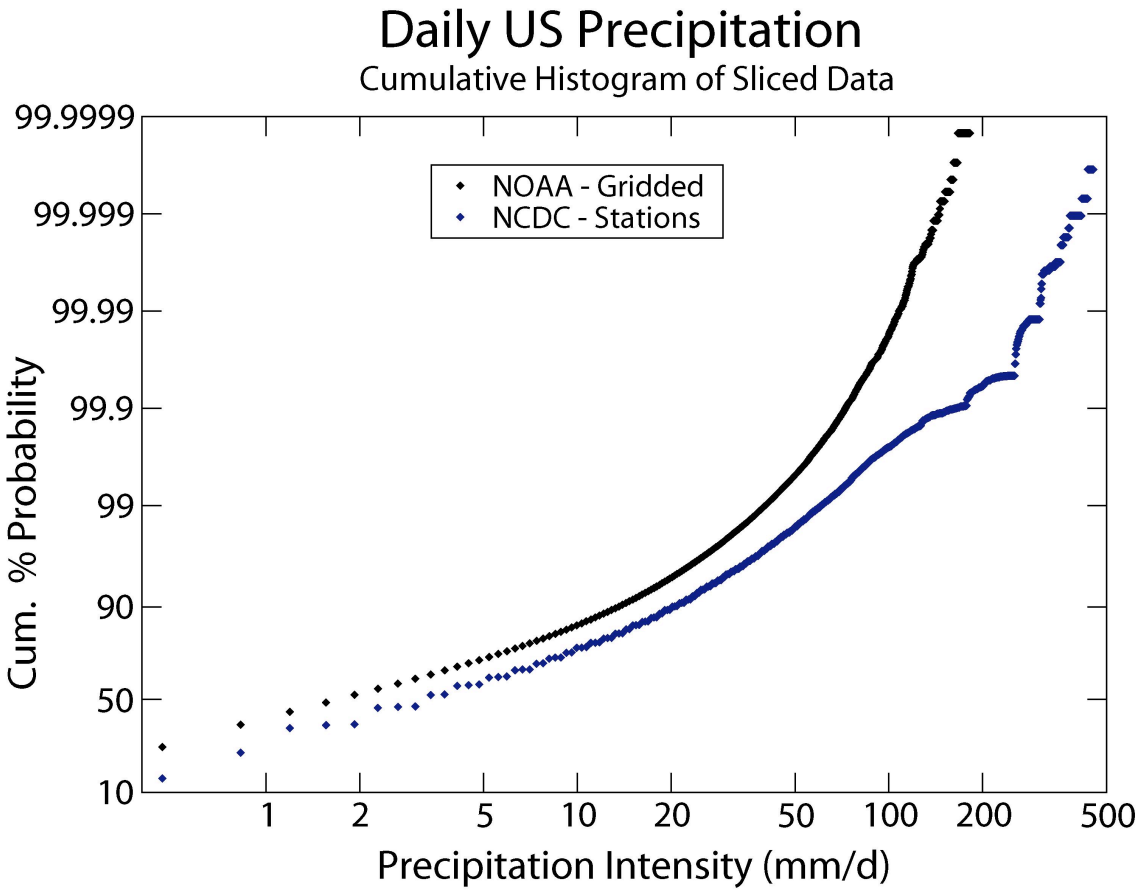
Daily US Precipitation
Cumulative Histogram of Sliced Data
NOAA - Gridded
NCDC - Stations
Cum. % Probability
99.9999
99.999
99.99
99.9
99
90
50
10
1
2
5
10
20
50
100
200
500
Precipitation Intensity (mm/d)

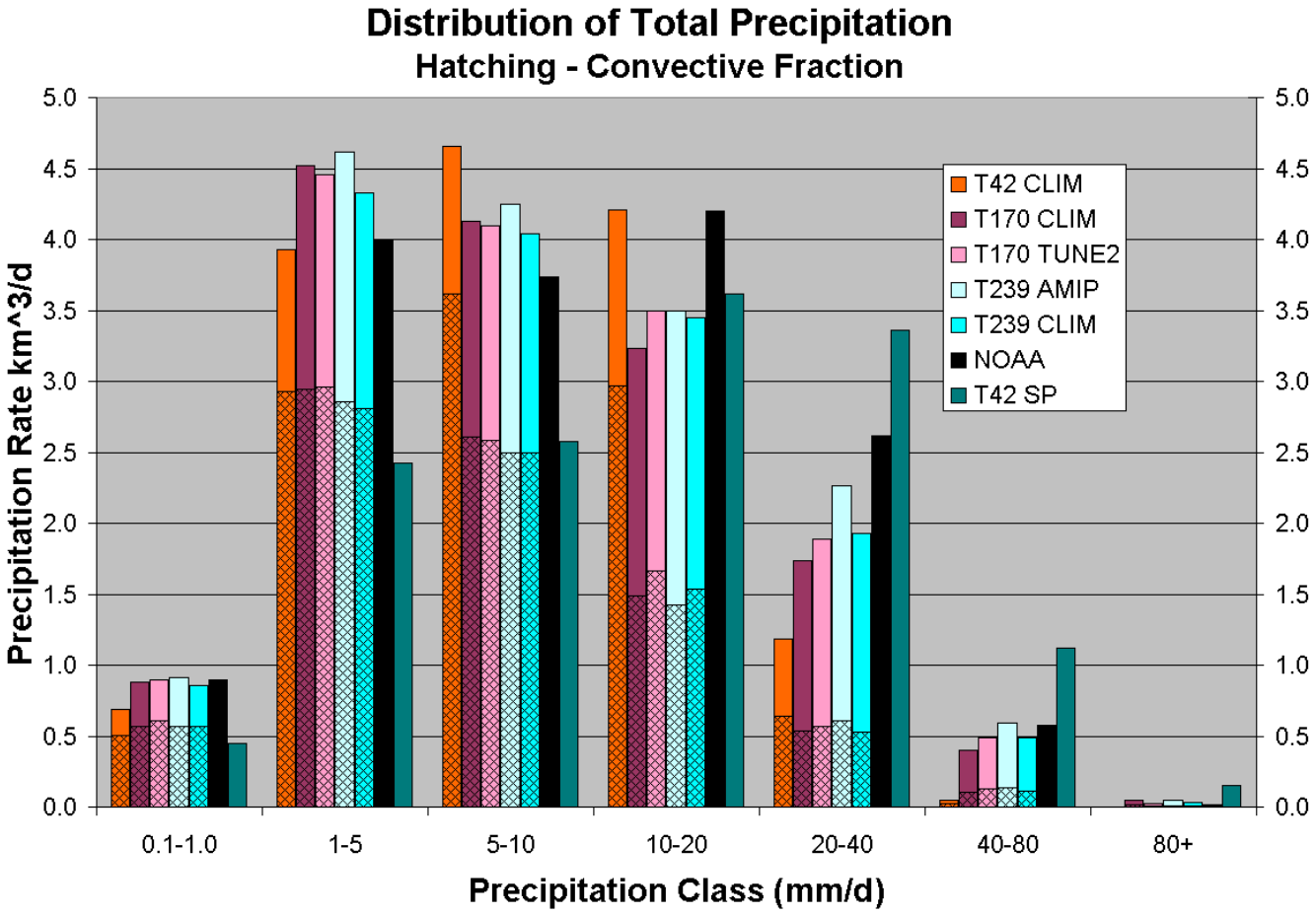
Distribution of Total Precipitation
Hatching - Convective Fraction
Precipitation Rate km^3/d
5.0
4.5
4.0
3.5
3.0
2.5
2.0
1.5
1.0
0.5
0.0
T42 CLIM
T170 CLIM
T170 TUNE2
T239 AMIP
T239 CLIM
NOAA
T42 SP
0.1-1.0
1-5
5-10
10-20
20-40
40-80
80+
Precipitation Class (mm/d)

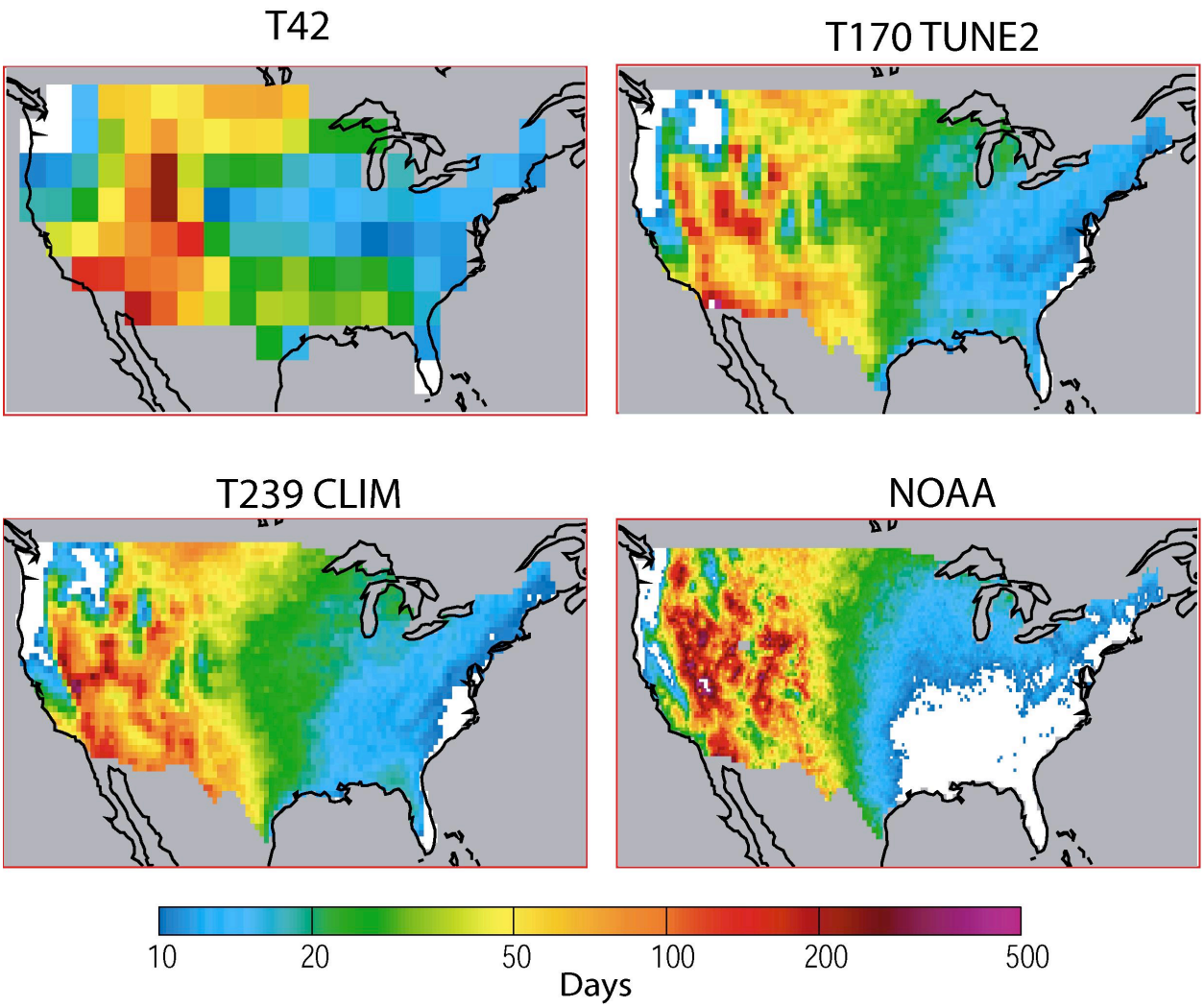
T42
T170 TUNE2
T239 CLIM
NOAA
10
20
50
100
200
500
Days

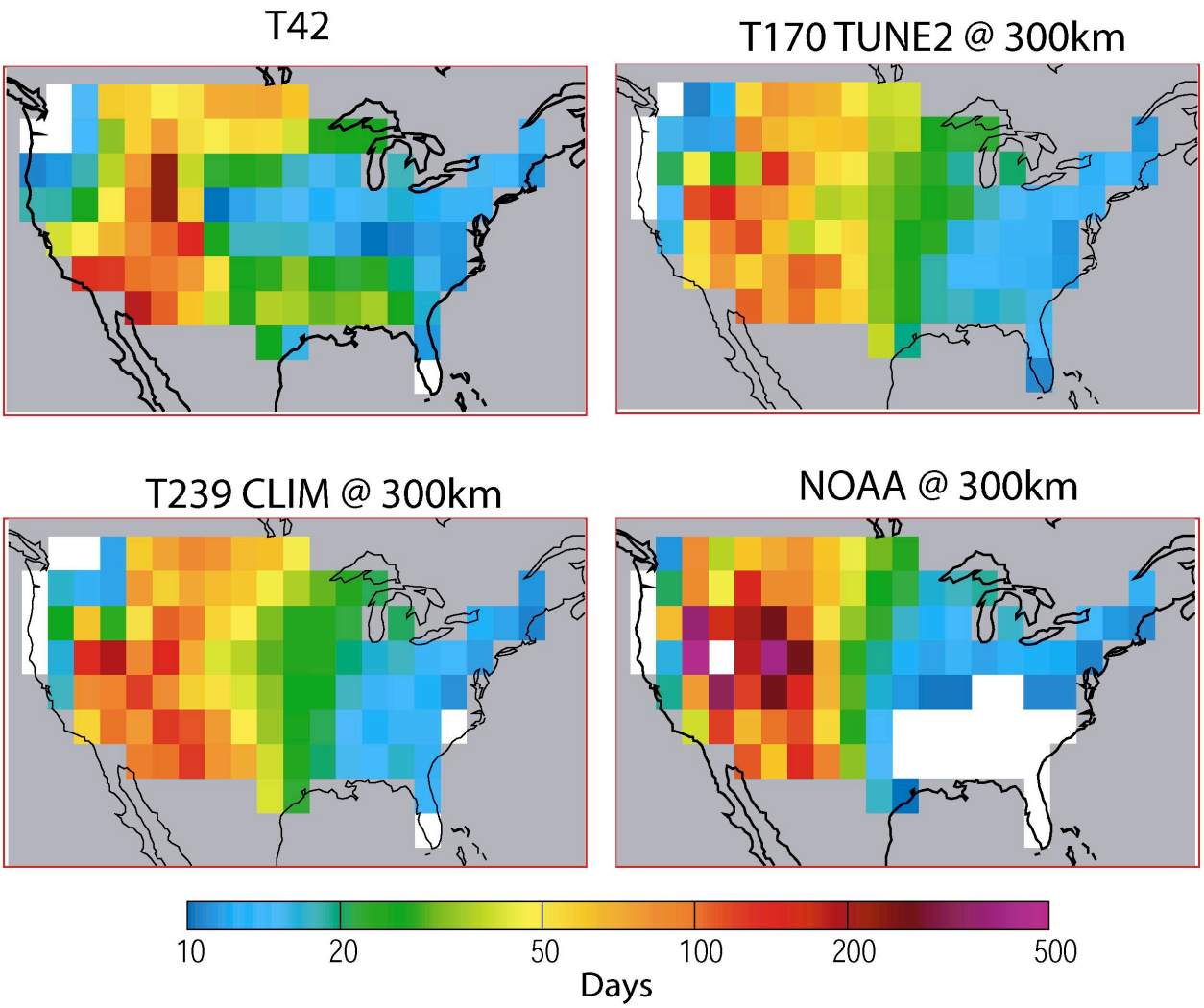
T42
T170 TUNE2 @ 300km
T239 CLIM @ 300km
NOAA @ 300km
10
20
50
100
200
500
Days

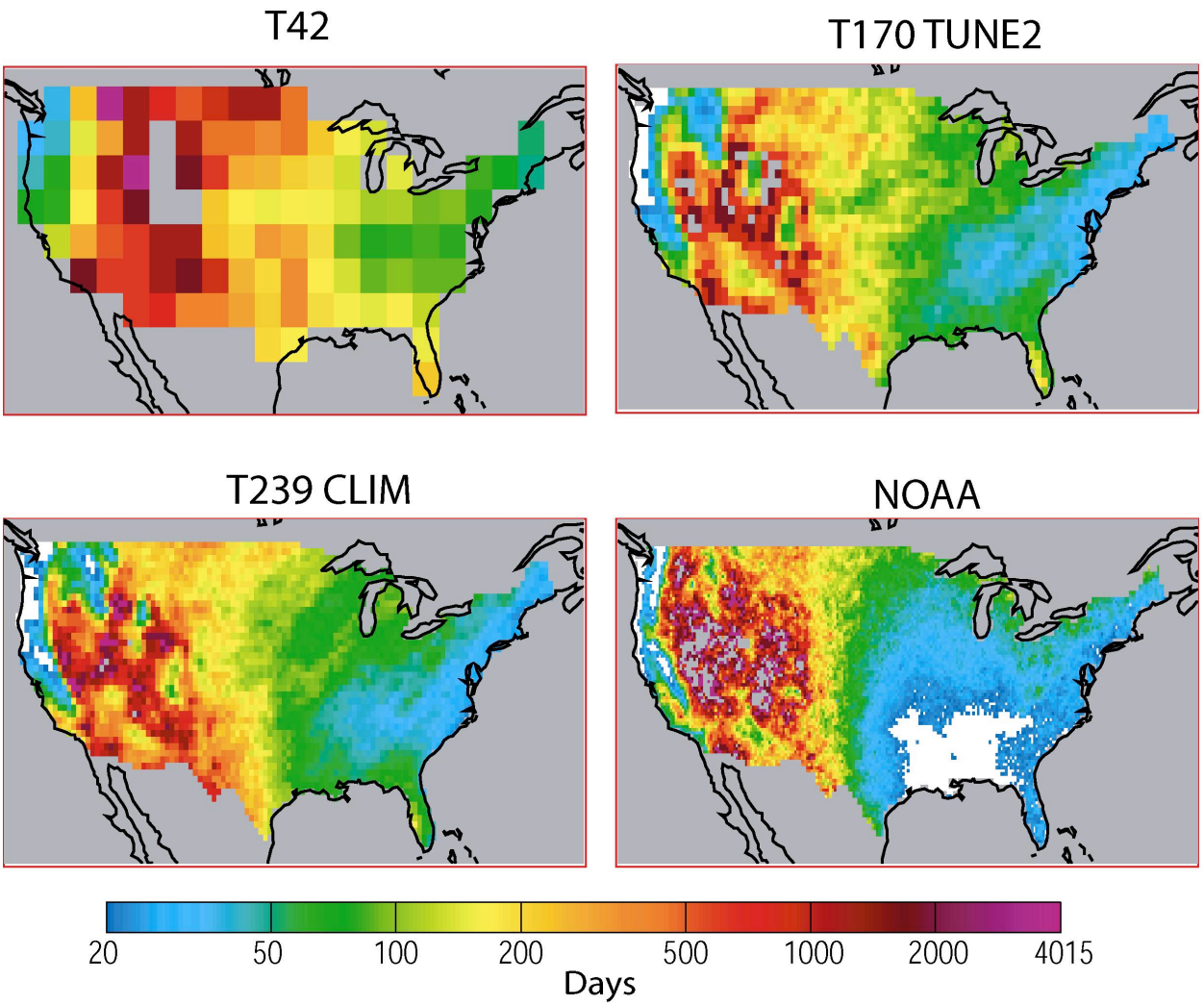
T42
T170 TUNE2
T239 CLIM
NOAA
20
50
100
200
500
1000
2000
4015
Days

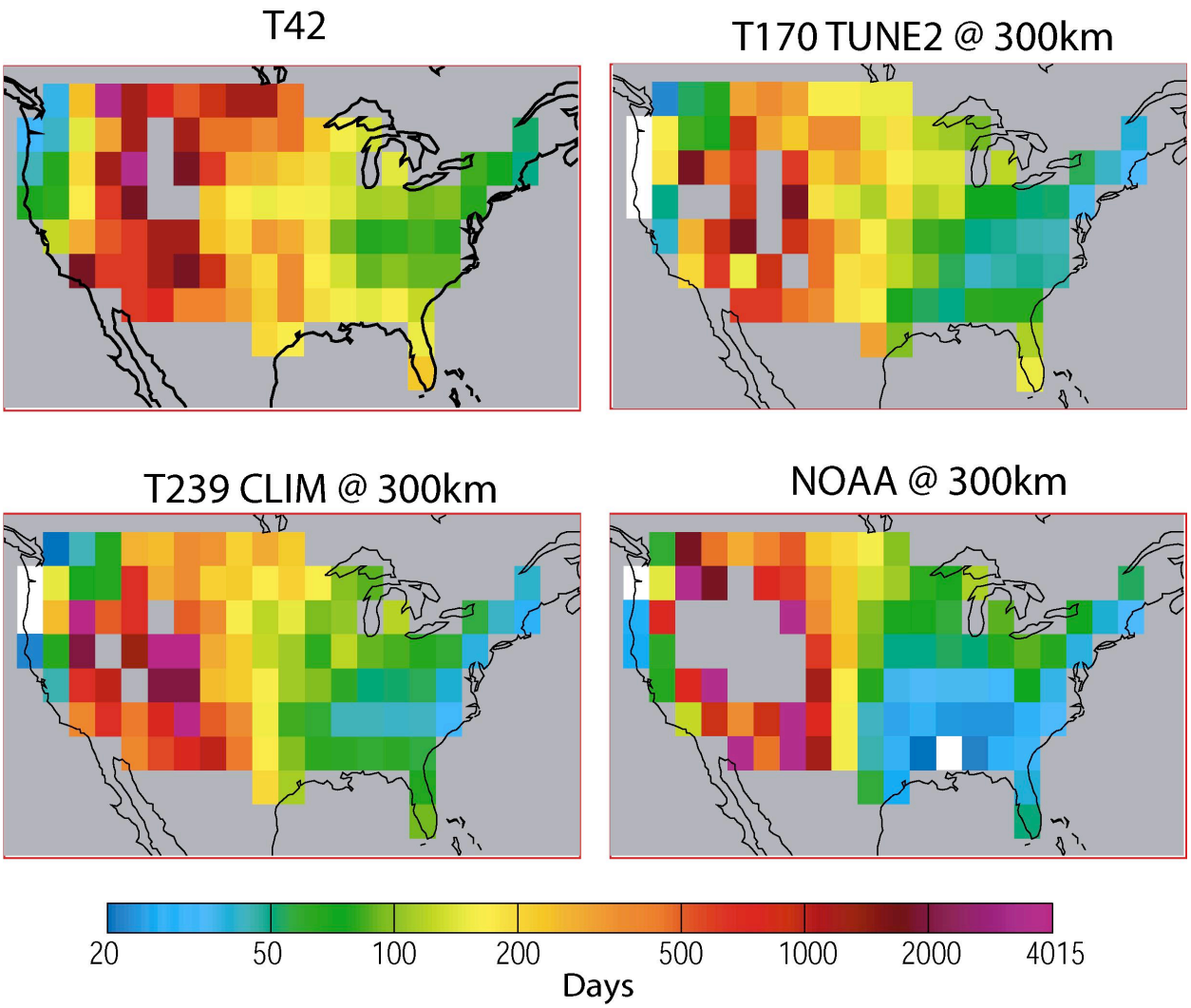
T42
T170 TUNE2 @ 300km
T239 CLIM @ 300km
NOAA @ 300km
20
50
100
200
500
1000
2000
4015
Days

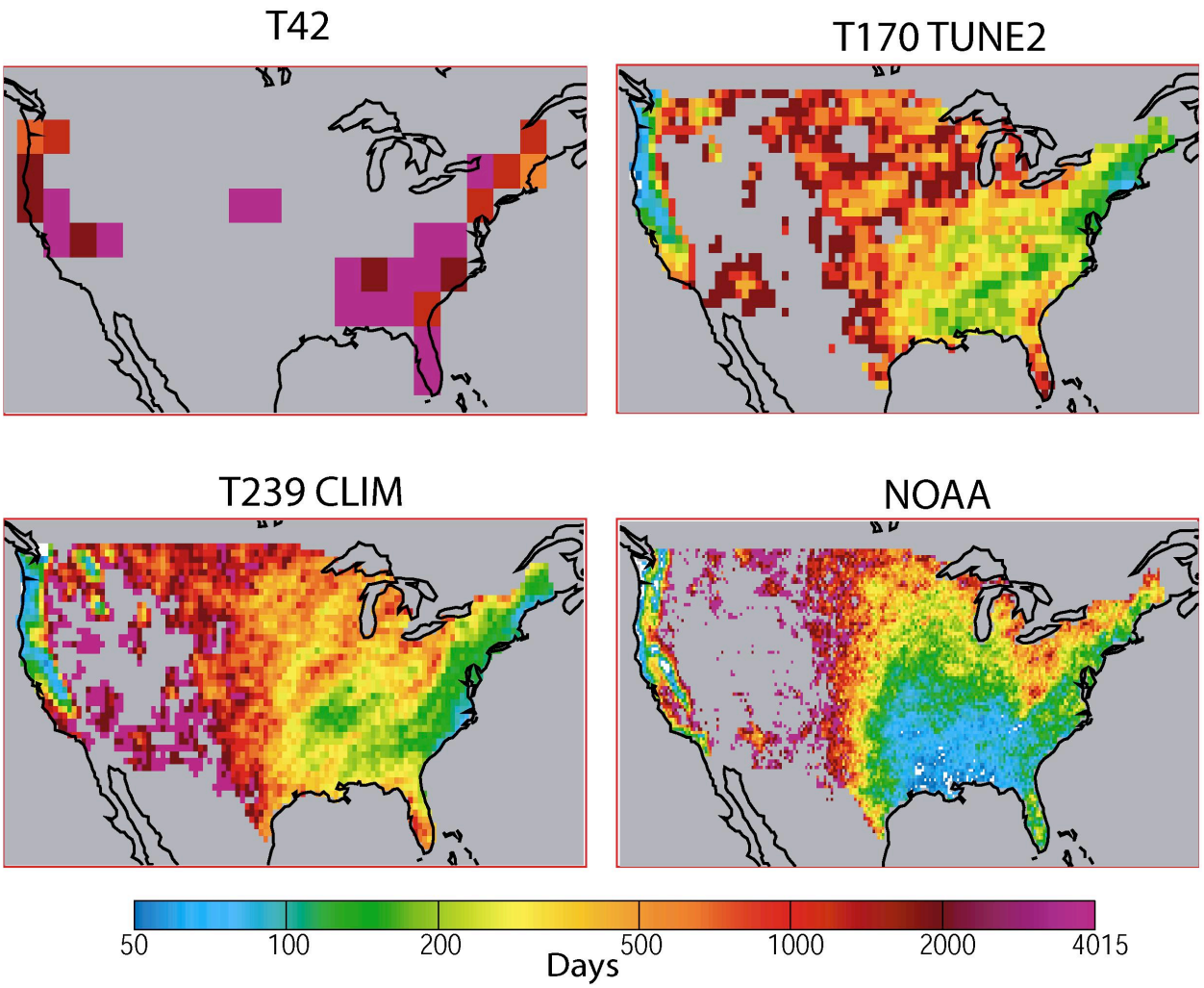
T42
T170 TUNE2
T239 CLIM
NOAA
50
100
200
500
1000
2000
4015
Days

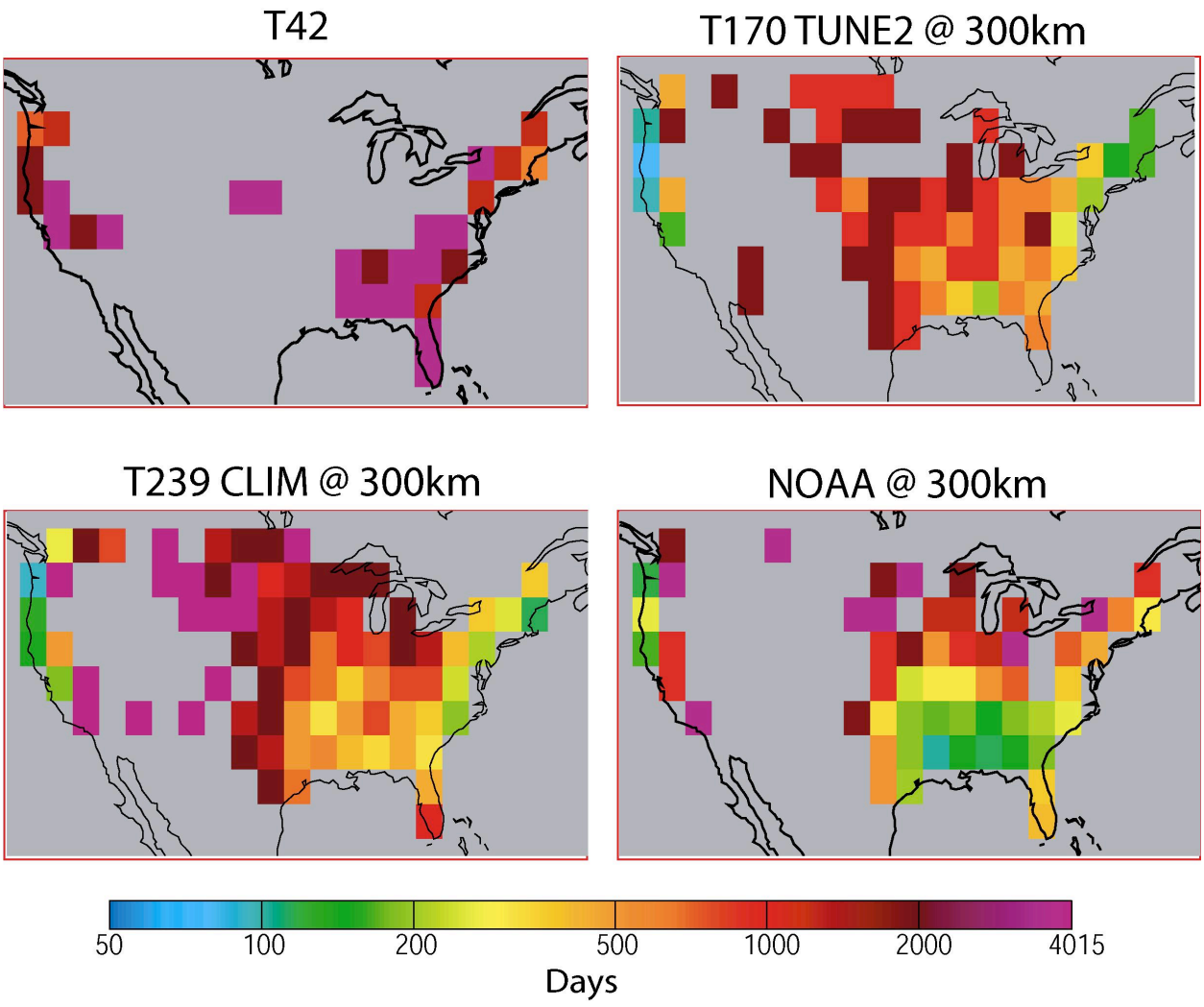
T42
T170 TUNE2 @ 300km
T239 CLIM @ 300km
NOAA @ 300km
50
100
200
500
1000
2000
4015
Days

University of California
Lawrence Livermore National Laboratory
Technical Information Department
Livermore, CA 94551